*mining*

MDPI

*Article*

# Sedimentological Controls on Stratabound Copper Mineralisation in the Ediacaran Tabia Member (Western Anti-Atlas, Morocco)

**Mouad Benssaou [1], Atmane Madi [2], Abdelilah Benhammou [2], Mohamed Abioui [3,*], Nourissaid Içame [1], Mehdi Ousbih [4], Ahmed Elmouden [1], Abderrahmane Wanaim [3], Hassan El-Baghdady [3] and Moha Ikenne [1]**

1 LAGAGE Laboratory, Department of Earth Sciences, Faculty of Sciences, Ibnou Zohr University, Agadir 80000, Morocco; mouad.benssaou.60@edu.uiz.ac.ma (M.B.); n.icame@uiz.ac.ma (N.I.); a.elmouden@uiz.ac.ma (A.E.); m.ikenne@uiz.ac.ma (M.I.)
2 MANAGEM Group, Casablanca 20250, Morocco; a.madi@managemgroup.com (A.M.); a.benhammou@managemgroup.com (A.B.)
3 GEG Laboratory, Department of Earth Sciences, Faculty of Sciences, Ibnou Zohr University, Agadir 80000, Morocco; a.wanaim@uiz.ac.ma (A.W.); hassan.elbaghdady.78@edu.uiz.ac.ma (H.E.-B.)
4 L3GA Laboratory, Department of Geosciences, Faculty of Sciences and Techniques, Moulay Ismail University, Errachidia 52000, Morocco; m.ousbih@umi.ac.ma
* Correspondence: m.abioui@uiz.ac.ma

## Abstract

In the Western Anti-Atlas, the stratiform copper mineralisations of the Tabia Member are distinctly hosted within sedimentary rocks, forming deposits comparable to the sediment-hosted stratabound copper (SSC) type. In Tizert, Ouarmdaz, and Talat n'Ouamane, the sandstones and clays host primary sulphides as disseminations and copper carbonates occurring as small continuous or lenticular beds, small geodes, and coatings on clay laminations. In Tiferki, the conglomerates are more mineralised; sulphides are represented by chalcopyrite and bornite, locally altered into chalcocite. Copper carbonates appear as malachite and azurite coating pebbles and deeply impregnate the granular matrix. From a sedimentological and sequence-stratigraphic perspective, the conglomeratic level at Tiferki represents a low-sea-level prism (LST) formed during a stage of maximum platform exposure allowing erosion products to accumulate at the base of the slope. By contrast, the silty–sandy complex known as the "Talat n' Ouamane level" corresponds to a prograding sedimentary sequence (Highstand Systems Tract, HST) that developed after a relative regression where the platform was only partially exposed. In both cases, relative sea-level fall promoted the emergence of the hinterland and active erosion, supplying the depositional environment with coarse detrital during the maximum drops in sea level and sandy-to-micro-conglomeratic deposits during less pronounced regressions. This detrital supply probably brought copper in the form of grains and especially dissolved copper, which is largely deposited at the bottom of slopes and in marine environments where microbial communities contribute to the precipitation of copper. The selective distribution of sulphides within the Tabia Member shows that only the low-sea-level and high-sea-level prisms are enriched in stratiform copper, while the transgressive and maximum flooding systems tracts lack significant mineralisation. This suggests that sea-level variations played a controlling role in copper deposition. The regressive trend of the high sea-level suite continued until emergence, reflected by the invasion of the environment by red or ochre siltstones from the alluvial plain. The emergence at the transition from sandstones to dolomites, and the "Red Beds"-type mineralisation embedded in these subaerial facies, support the syngenetic origin of the sulphides in the Tabia Member. After this main emplacement of stratiform copper, the sulphides would have undergone remobilisation

Check for updates

Academic Editors: Jingshou Liu, Wenlong Ding, Lei Gong and Ang Li

Received: 9 June 2026
Revised: 23 July 2026
Accepted: 30 July 2026
Published: 4 August 2026

**Copyright:** © 2026 by the authors. Licensee MDPI, Basel, Switzerland. This article is an open access article distributed under the terms and conditions of the Creative Commons Attribution (CC BY) license.

and alteration during a significant episode of vertical water escape that deformed the host facies and enhanced mineral concentration within permeable sandstones. Even the clays were delaminated and coated with a thin films of copper carbonates on their surfaces. In the Tamjout dolomites, carbonates are percolated by acidic solutions, contributing to the brecciation and silicification of the stromatolitic layers. Copper mineralisation accompanies this silicification and fills the karstification pockets.

**Keywords:** sediment-hosted stratabound copper (SSC); sea level change; Ediacaran Tabia Member; microbial community; soft-sediment deformation; Anti-Atlas

## 1. Introduction

Stratiform copper, referred to as sediment-hosted stratabound copper (SSC), are copper ore bodies stratified within detrital sedimentary rocks (conglomerates, sandstones, siltstones, mudstones, and other clastic rocks) [1–3]. They represent the second largest accumulation of copper worldwide, exceeded only by the porphyry type [1,3]. Although SSC accounts for a substantial portion of known copper resources (up to 30%), economically viable deposits are rare [4]. While most studies acknowledge the occurrence of SSC in intracontinental basins undergoing extension, the mechanism of their formation remains controversial because the timing of copper sulphide precipitation relative to host sedimentation and the duration of mineralisation are not unanimously agreed upon. Indeed, the primary genetic models proposed generally range between diagenetic and epigenetic processes, with sedimentogenetic models being rarely invoked:

- Diagenesis is considered the principal mechanism for the formation of copper mineralisation, as exemplified by the Luiswishi and Kamoto deposits in the Katanga Copperbelt of the Democratic Republic of Congo and Zambia [5]. In these deposits, copper–cobalt sulphide ores formed during early diagenesis of the host sediments, consistent with the widespread stratiform mineralisation seen in this region. The diagenetic process can occur after shallow burial, where reducing conditions, including bacterial sulfate reduction, promote the precipitation of sulphide minerals, or later at greater burial depths without exceeding roughly 1000 m, with early diagenetic sulfur phases being replaced during continued chemical evolution. Late diagenetic adjustment and remobilisation of sulphides can be recognised where mineralisation extends the primary host facies into adjacent strata.
- Epigenesis, which comes in second, corresponds to telogenesis, meaning that mineralisation occurred after the host facies was brought back to the surface by tectonic inversion of the basin. Model examples include the copper-belt deposits in Central Africa [6] and the Nussir deposit in the Norwegian Arctic [7].
- Sedimentogenesis, which is rarer, is expressed either by the direct detrital input of copper into the depositional area, as documented in the Jiashi area basin, northwestern China, where Paleogene clastic strata received copper-rich detritus derived from weathered source rocks [4], or in the form of dissolved copper that precipitates in situ when reducing conditions develop in organic-rich or low-oxygen pore waters.

However, the genesis of stratiform copper is rarely attributable to a single mechanism, as sedimentary basins typically experience a superposition of geodynamic events throughout their geological history. Consequently, the formation of SSC-type deposits is often polyphase and multimodal. This is well illustrated by the Jiashi Basin in northwestern China [4], where detrital copper underwent alteration followed by remobilisation due to hydrodynamic and weathering processes induced by tectonic events. A similar evolution

characterises the diagenetic deposits of Central Africa, including those of the Katanga region in the Democratic Republic of Congo, which were subsequently remobilised by tectonic processes [5,8].

In Morocco, copper deposits have significant typological diversity, depending on the lithological nature of their host rocks. Sediment-hosted copper mineralisation is documented in several geological settings: (i) the Paleoproterozoic of Bleida [e.g., [9–12]]; (ii) the Cryogenian Tidiline Formation of the Bouazzer-El Grara inlier [13,14]; (iii) the Tabia Member of the Adoudou Formation (Ediacaran–Cambrian transition?) of the Western Anti-Atlas [15–19]; (iv) the Cambrian cover of the Bouazzer inlier [20–22]; and (v) the Ordovician of Oumjrane [23]. Among these occurrences, the copper deposits associated with the Ediacaran–Cambrian transition (Tabia Member) are particularly noteworthy. They are hosted in conglomerates, sandstones, siltstones, and clays, and locally in carbonates, and they fully satisfy the criteria of sediment-hosted stratiform copper (SSC-type) deposits. The maximum copper mineralisation is concentrated within siltstone and sandstone horizons immediately underlying the Tamjout dolomites (Tifnout Member), a mineralised interval referred to by Pouit [17] as the Talat n'Ouamane Level (TOL). A distinctive feature of the TOL is its extensive geographical distribution, covering the Igherm, Ouaoufengha, Ait Abdallah, and large portions of the Kerdous (Agoujgal) inliers. This regional continuity has led to the development of several major copper deposits, some of which are currently active (e.g., Tazalaght, Tizert, Amadouz), while others are abandoned or temporarily inactive (e.g., Tiferki, Talat n'Ouamane, Agoujgal). Among these, the Tizert deposit is the most significant, with estimated reserves of 56.82 million tonnes [18]. The TOL is not the sole stratigraphic horizon hosting stratiform copper mineralisation. Copper occurrences are also reported within the overlying Tamjout dolomites and the underlying basal conglomerates, notably in the Tanguerfa inlier [24] and the Tiferki area. The genesis of these cupriferous levels has been the subject of long-standing debate, leading to the development of several genetic models concerning both the origin and the mechanisms of mineral deposition. Some authors consider the Cambrian copper accumulations as diagenetic in origin, while others argue for an epigenetic or purely syngenetic genesis. Bourque et al. [21], for example, emphasise the metallogenic complexity of the Anti-Atlas and propose an epigenetic model involving fluid circulation within the Adoudou, Igoudine, Issafène, and Amouslek formations of the Bou Azzer inlier. This model may also explain stratabound copper mineralisation in the basal series of the Western Anti-Atlas. In contrast, Pouit [17] and Oummouch et al. [18] advocate a syngenetic or diagenetic origin, supported by a pronounced spatial distribution in which the largest copper concentrations occur along the margins of extensive depressions surrounded by paleo-reliefs. While Pouit [17] reported the presence of detrital copper grains within the TOL, Oummouch et al. [18] favour a diagenetic precipitation of sulphide minerals. Indeed, in the Tizert area, drilling data reveal the existence of primary sulphides disseminated in sandstones, siltstones, and rarely microconglomerates [18]. The main established parageneses differ from one basin to another and even differ from one zone to another within the same basin, but the maximum mineralised thickness is found near the paleo high. The mineralised body always shows bornite and chalcocite at the base in a coarse-grained sediment and chalcopyrite and framboidal pyrite at the top where the sediment becomes fine (siltites). Laterally, bornite and chalcocite predominate near the paleo-high, while chalcopyrite and pyrite are more common further from the reliefs. They further note that the concentration of disseminated copper is proportional to the pore size of the host sediment. These same parageneses are found in small pockets of karstification within the carbonates of the Tamjout dolomites and in fractures which affect the basal series indifferently. In addition to primary sulphides, secondary minerals such as chalcocite develop at the expense of pyrite and chalcopyrite, whereas supergene

alteration to copper carbonates is restricted to the outer envelopes of the mineralised bodies. Unlike primary sulphides, alteration mineralisation shows a clear transgression across the different lithologies of the basal series. However, this altered belt has also been the subject of detailed petrographic and geochemical investigations, which confirmed the absence of primary sulphides and the dominance of malachite within the Tamjout carbonates and the uppermost clay-rich levels of the Tabia Member [25]. The results of these studies are integrated into the discussion of our findings. Ouchchen et al. [19], based on a geophysical investigation, further confirm the occurrence of mineral concentrations near paleo-reliefs, where northeast-trending faults serve as conduits for mineralising fluids, although without explicitly defining the genetic mechanism. These authors even suggest the possibility of mineralisation deposition, or at least a tectono-thermal remobilisation, in connection with the Central Atlantic Magmatic Province (CAMP). However, none of the proposed models explains the coexistence, within a single deposit, of layered, disseminated, fissural, karst-related mineralisation styles. What all existing models have in common is their reliance on mineral paragenesis as the principal criterion for genetic interpretation. Other factors, such as tectonic structures, fluid inclusions, geochemistry signatures, and geophysical data, are considered. Sedimentological facies analysis and sequential stratigraphy have never been applied at a local scale to elucidate the relationship between depositional environments and mineralisation. Such an approach can, however, provide valuable insights into whether the factors controlling the development of host facies also influence the genesis of stratiform copper deposits. The effectiveness of this methodology has been demonstrated in previous studies. McConachie and Dunster [26] showed that stratiform mineralisation commonly concentrates within lowstand and highstand marine prisms. Ruffell et al. [27] proposed a sequence-stratigraphic model highlighting mineral concentration during Highstand Systems Tracts, whereas Shi et al. [4] demonstrated that lowstand systems can also favour the concentration of detrital copper.

In this study, we apply sedimentological and sequence-stratigraphic analyses to provide new insights into the ongoing debate concerning the formation of stratiform copper mineralisation within the Tabia Member and the Tamjoute dolomites. This approach aims to clarify the potential relationship between the sedimentary dynamics and mineralisation distribution, to improve mineral exploration targeting. Consequently, this work does not constitute a classical metallogenic study based on petrography, geochemistry, and mineral parageneses, but rather a focused analysis of the primary depositional signature expressed through facies and stratigraphic sequences. Indeed, morphological features such as large-scale stratification and sedimentary structures, as well as architectural organisation, are relatively insensitive to diagenesis, which preferentially affects texture and mineralogy. Facies and sequence analysis can therefore provide additional genetic information that classical approaches (petrography, paragenesis, and geochemistry) are often unable to reveal.

## 2. Geological, Geomorphological and Geodynamic Framework

The Anti-Atlas is a mountain-belt oriented SW-NE to WSW-ENE, uplifted along the northern margin of the West African Craton (WAC) (Figure 1). It extends for approximately 660 km, from the Atlantic Ocean in the west to the Guir Hamada in the northeast. This region, composed of several Proterozoic inliers, constitutes a key geological transition between the Saharan domain, where Archean formations crop out in the Rguibates Shield, and the younger Variscan to Alpine domains in the north, represented by the Meseta, the High and Middle Atlas, and Rif belts [28].

Structurally, the Anti-Atlas is bounded to the north by the South Atlas Fault (SAF) and gradually disappears under the Cretaceous and Plio–Quaternary deposits (Figure 1). To the

south–central part, it is traversed by the Anti-Atlas Major Fault (AAMF), which juxtaposes a southwestern Paleo-Proterozoic domain against a northeastern Neoproterozoic domain. From a geodynamic perspective, the Anti-Atlas underwent two major tectono-metamorphic and magmatic events: (i) the Eburnean orogeny, dated between ca. 2.25 and 1.98 Ga; and (ii) the Pan-African orogeny, between ca. 780 and 545 Ma. In addition, the region records weaker but significant geodynamic events during the Paleozoic (Variscan orogeny), the Mesozoic (Triassic extension and emplacement of Jurassic dike swarms), and the Cenozoic, during which reactivation of faults and basement exhumation occurred in relation to Alpine tectonics [29]. In the western Anti-Atlas (Figure 1), the principal tectonic windows are those of Kerdous, where the basement is dominated by granites and quartzites, and Igherm, characterised by conglomerates and volcano–sedimentary rocks of the Neoproterozoic Ouarzazate Group. The Ighrem inlier constitutes the focus of this study, as its sedimentary cover hosts significant stratiform copper mineralisation, mainly concentrated within the lower lithostratigraphic levels of the Adoudou Formation.

Stratigraphically, these levels correspond to the Ediacaran–Cambrian transition, or possibly remain entirely Ediacaran, since the formal Ediacaran–Cambrian boundary (541 Ma) is not located at the top of the Tabia Member but rather above the Tamjout dolomites [30,31]. Importantly, this geological interval coincides with the onset of Cambrian rifting in the Anti-Atlas, which led to the development of an extensive shallow carbonate platform dominated by microbial communities [32]. It is therefore interesting to investigate whether these geodynamic and biological conditions played any role in controlling the formation and distribution of the stratiform copper mineralisation contained in the Tabia Member and the Tamjout dolomites.

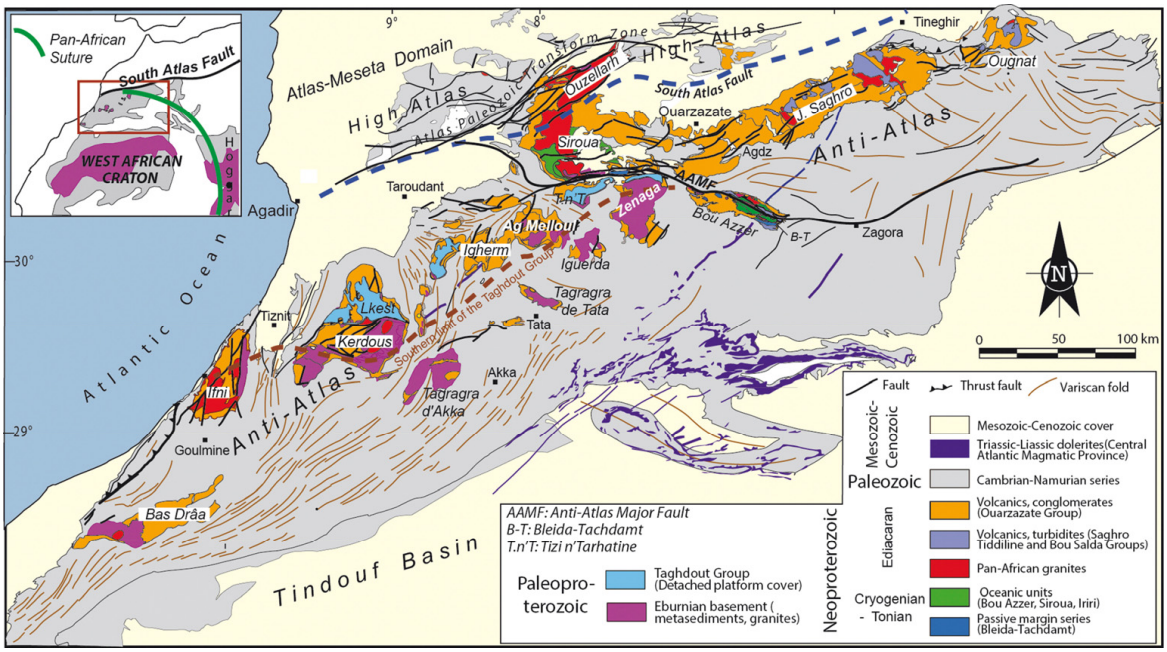



**Figure 1.** Simplified geological map of the Anti-Atlas (after Gasquet et al. [33], slightly modified after Soulaimani et al. [34]). In the box—location of the Anti-Atlas domain north of the West African Craton (WAC).

## 3. Materials and Methods

This study, conducted both in the field and at the Tizert mine headquarters, focused on the examination of borehole cores from three wells in the Tizert region (Tiz C237, Tiz 208, and Tiz C 459), provided by the MANAGEM Group. This was complemented by detailed stratigraphic sections measured at the Tizert, Tiferki, Ouarmdaz, and Talat open-pit mines

(Figure 2). During the fieldwork, additional samples were collected and a comprehensive photographic record was established.

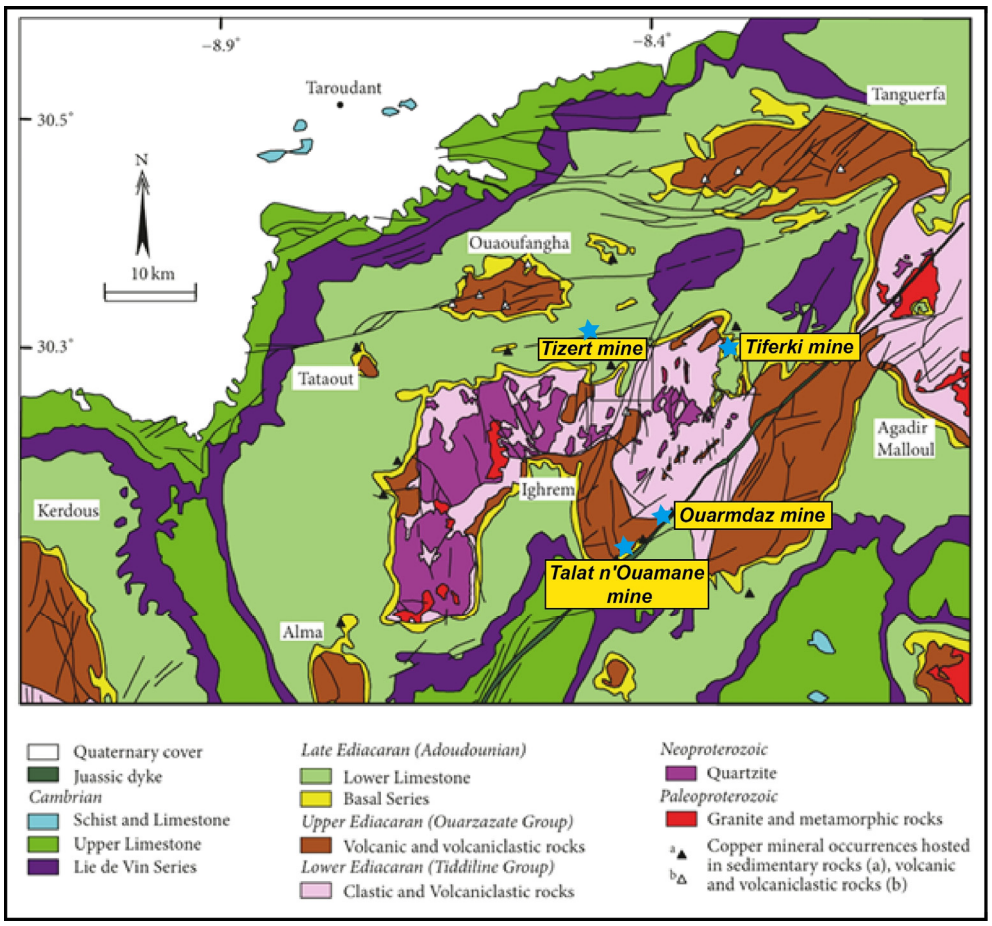



**Figure 2.** Geological and structural map of the Taroudant–Igherm inlier (1/100,000 geological map of Taroudant–Igherm, 1983; modified from Oummouch et al. [18]). Blue asteroid presents the location of the mines discussed in this paper.

Borehole cores were examined over a four-day period, and their compilation enabled the reconstruction of stratigraphic logs for each well. Consequently, a column of approximately 70 m was reconstructed for borehole Tiz 208, and approximately 100 m for both Tiz C237 and Tiz C459. Representative samples were prepared as petrographic thin sections at the Thin Section Workshop of the Department of Earth Sciences, Faculty of Sciences, Ibnou Zohr University, Agadir, Morocco. Forty thin sections were initially examined by optical microscopy but only two of them were subjected to detailed analysis using a JEOL IT510LV InTouchScope™ Scanning Electron Microscope (JEOL Ltd., Akishima, Tokyo, Japan), operating at an accelerating voltage of 20 kV with a count rate of 4120 cps.

Data interpretation is based on facies sedimentology and sequence stratigraphy. Given that the majority of the deposits studied here are detrital in origin and devoid of fossils, sedimentary structures provide the primary basis for facies identification. Within the sandy intervals, the internal bedding laminations are well-developed. Several types of laminated structures occur, each recording specific hydrodynamic conditions. The characterisation of these laminated structures relies on several parameters [35–37], including: (i) the geometric relationship between the internal laminations and the bed boundaries; (ii) the direction, orientation, and dip angle of the laminae; (iii) the planar or arcuate fabric of the laminae; and (iv) the distribution of laminae based on thickness, lithology, and colour.

In conglomeratic facies, internal lamination is less apparent; however, other criteria, such as clast texture, shape, and petrological composition, enable facies identification and interpretation [38,39]. Whether sandy, conglomeratic, or clayey, an individual facies only permits the reconstruction of local depositional mechanisms. Reconstructing the broader depositional environment requires analyzing the combination of facies and architectural elements [38].

Sequence stratigraphy is utilised to identify stratigraphic sequences that record the geodynamic evolution of the basin over time. As the primary method for analyzing ancient sedimentary series, it is based on the concept of accommodation space, which is created or reduced by relative sea-level changes. This space, in turn, is controlled by the interplay of eustasy, sediment flux, and tectonic and thermal subsidence.

The systems tract nomenclature used here follows that proposed by Catuneanu [40]. Thus, the acronyms HST, TST, LST, and FSST represent the Highstand Systems Tract, Transgressive Systems Tract, Lowstand Systems Tract, and Falling-stage Systems Tract, respectively. Notably, the HST, LST, and FSST are all categorised as regressive systems tracts [40].

By applying this integrated sedimentological approach, it is possible to define the systems tracts associated with each stage of relative sea-level change, ultimately determining which of these tracts host mineralisation. From a metallogenic perspective, the published literature, specifically data from Oummouch et al. [18] and Poot et al. [25], is integrated to enrich the discussion.

## 4. Results

### *4.1. Tiferki Quarry*

#### 4.1.1. Description of Facies and Sequences

At Tiferki, the sedimentary succession is dominated by conglomeratic, microconglomeratic, sandstone, and siltstone deposits. Five distinct facies have been identified:

- Facies Tif1 (Figure 3a,b) consists of rounded pebbles supported by a friable, grayish sandstone matrix. The pebbles are variable in size, up to 20 cm in diameter, and are generally dispersed within the matrix without any apparent internal structure. The basal contact of this facies is highly irregular and erosional (Figure 3a), overlying a well-consolidated, reddish, volcanic-pebble conglomerate. Notably, facies Tif1 contains isolated quartz diorite pebbles, which exhibit complete alteration in feldspars to micas under microscopic examination. These alteration micas likely constitute a major component of the clay-rich facies of the overlying Tabia Member. Dissolution spaces between feldspar phenocrysts within the quartz diorite are filled by irregular patches of titanium oxides (Figure 3e), which also occur as acicular crystals cross-cutting the feldspars (Figure 3f). Scanning electron microscopy (SEM) analysis indicates that these oxides consist of ilmenite containing more than 60% titanium (Figure 4a). Both the irregular and acicular titanium oxides are late-stage, likely resulting from hydrothermal activity that also facilitated the feldspar-to-mica alteration within the quartz diorite prior to its erosion. The oxides within interstitial spaces often contain relics of feldspars, micas, and small sulfate crystals, as revealed by SEM (Figure 4b,c). Within facies Tif1, copper occurs as chalcopyrite, chalcocite (Figure 3c), and a copper-bearing carbonate cement that heavily impregnates the microconglomeratic matrix, locally imparting a vibrant green and blue colouration (Figure 3d). In addition to this stratiform copper mineralisation, malachite coatings are locally observed along late fractures cutting across the conglomerates.
- Facies Tif2 and Tif3 (Figure 5a,b) form a heterolithic assemblage approximately 10 m thick. This unit is organised into horizontal, decimeter- to meter-scale beds separated by planar boundaries. Each bed displays normal grading, beginning with a basal microconglomeratic layer (Facies Tif2) that transitions upward into a massive, gray-

ish sandstone (Facies Tif3). This facies association lacks primary sulphides; copper mineralisation is restricted to supergene malachite impregnations along fractures (Figure 5a,b).

- Facies Tif4 consists of a gray, non-mineralised silty–clayey unit with a maximum thickness of approximately 2 m (Figure 5c). It is characterised by millimeter-scale silty to sandy laminae systematically alternating with clayey laminae of similar thickness.
- Facies Tif5 differs from facies Tif4 primarily in its reddish-to-ochre colouration. It forms a monotonous succession up to 3 m thick, composed of millimeter- to centimeter-scale laminae of fine sandstone and siltstone. This facies is intensely mineralised with iron/copper oxides, which are likely responsible for its distinct reddish hue (Figure 5d).

The vertical stacking of these facies defines a single megasequence (Figure 6), which is further subdivided into several elementary depositional sequences. Within this megasequence, four elementary sequences, or systems tracts, can be distinguished: the lowermost tract is represented solely by the coarser facies Tif1; the second consists of the alternating, stacked succession of graded beds composed of facies Tif2 and Tif3; the third interval is represented by the fine-grained facies Tif4; and the final, uppermost tract is composed entirely of facies Tif5.

#### 4.1.2. Interpretation

The absence of internal structures within the conglomeratic facies Tif1 makes its interpretation challenging, as similar deposits can occur in alluvial fans, submarine fans, beach ridges, and fan-deltas. In an alluvial fan setting, conglomeratic deposits typically represent debris accumulations at the base of a subaerial slope, resulting from the erosion of a hinterland lacking vegetation cover. Under these conditions, erosional processes yield large blocks and angular clasts, which may or may not be supported by a clay matrix [38,41,42]. In such a scenario, fragile clasts and blocks, such as those of the quartz diorite, would be well preserved rather than decomposing into sand and small pebbles rich in altered feldspars. Furthermore, the oxidising conditions prevailing in subaerial environments would prevent the preservation or early formation of the primary copper sulfides hosted within the conglomerates.

In fan-deltas, the proximal zone resembles an alluvial cone, whereas the distal zone typically consists of small-pebble conglomerates alternating with sandstones and microconglomerates [39]. This does not align with the Tiferki conglomerate, which is characterised by medium-sized, rounded pebbles heavily cemented by a sandstone matrix. Similarly, in coastal marine settings, beach ridges exhibit flattened pebbles arranged in an interlocking, clast-supported texture that generally lacks a matrix. Furthermore, beach-ridge conglomeratic layers typically alternate with sandstones displaying wave- and tide-generated structures [39], features that are entirely absent in the Tiferki conglomerates.

A submarine fan depositional model best explains the accumulation of these coarse deposits and provides the reducing chemical conditions necessary for the development of primary copper mineralisation during syngenetic or early diagenetic stages. In this environment, conglomeratic deposits form following shelf exposure triggered by a relative sea-level lowstand. The products of erosion are transported by fluvial systems over long distances, allowing the resistant clasts to become well-rounded. Given that the Tiferki conglomerate contains highly altered quartz diorite pebbles, these clasts were easily disintegrated during transport to form a gray sandstone matrix remarkably similar in colour to the source quartz diorite. Upon reaching the basin slope, the sediment gravity flow behaved as a cohesive debris flow where the pebbles were supported by a sandy matrix [43–47]. This texture likely underwent reorganisation during burial, where compaction of the sand-rich matrix brought the pebbles closer together, destroying any primary depositional structures. Consequently,

facies Tif1 is interpreted as a Lowstand Systems Tract (LST), which is overlain by turbiditic facies (Tif2 and Tif3). The primary sulfides (chalcopyrite and chalcocite) indicate copper precipitation under reducing conditions, whereas the malachite present in the cement and fractures represents supergene alteration and subsequent remobilisation.

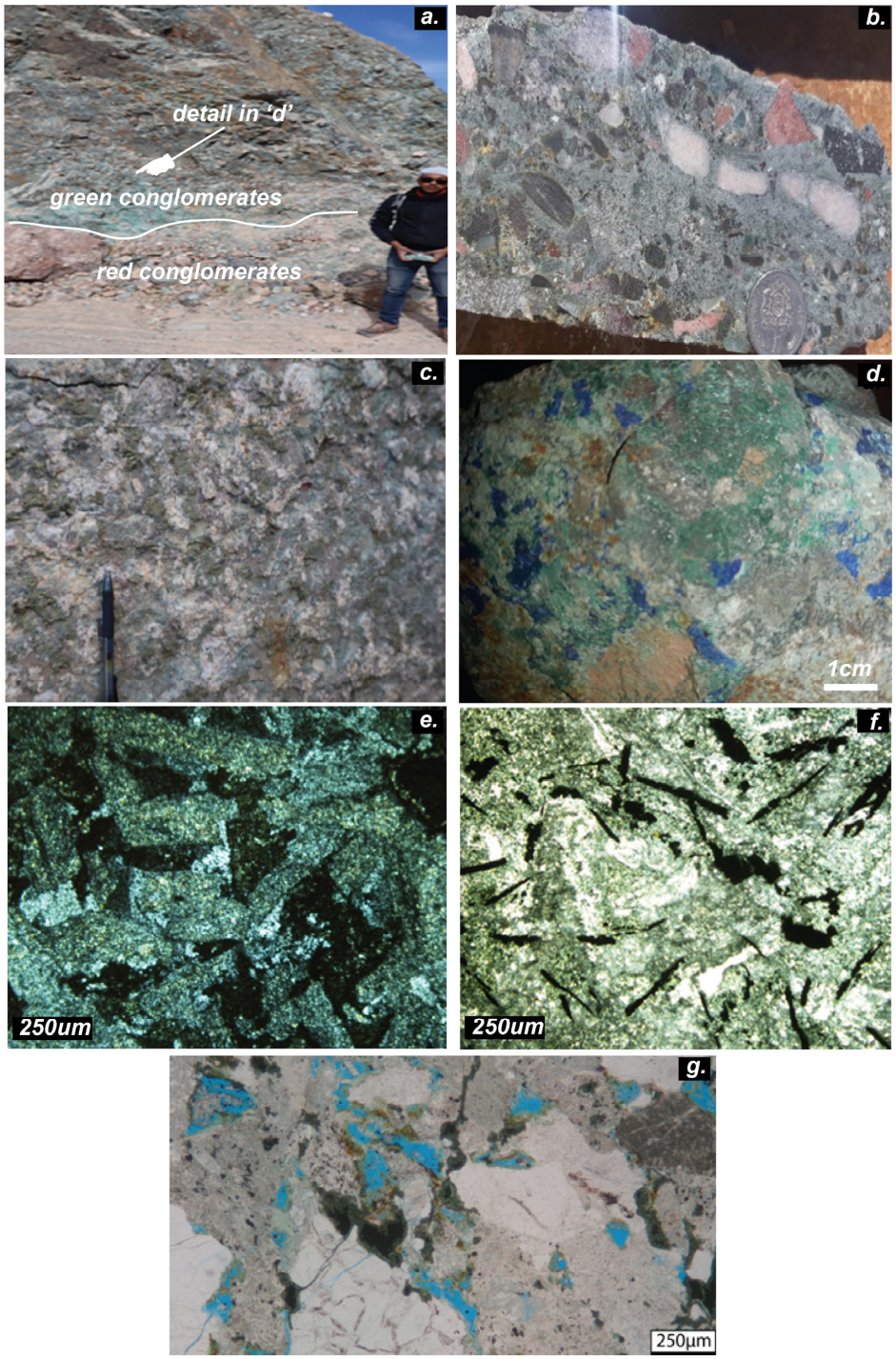



**Figure 3.** (**a**,**b**) Mineralised conglomeratic facies (Tif1); (**c**) sulphides (chalcopyrite; chalcocite) in mineralised conglomerates; (**d**) malachite and azurite disseminated in the sandstone matrix of conglomerates; (**e**) photomicrograph showing crystallised oxides between altered feldspars of quartz diorite; (**f**) photomicrograph showing the oxides in the form of acicular crystals intersecting feldspars; and (**g**) photomicrograph showing copper-bearing cement dispersed in the sandstone matrix of the conglomerates.

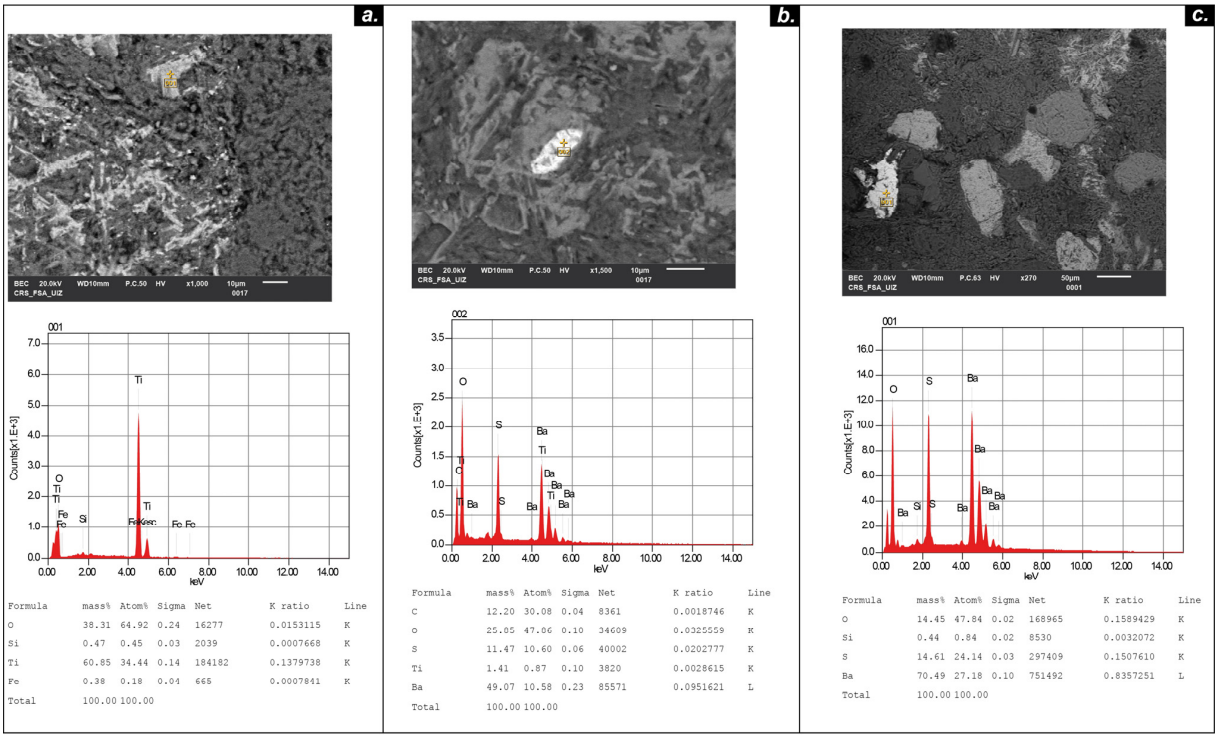



**Figure 4.** SEM analysis of ilmenite from quartz diorites (**a**), a crystal included in ilmenite (**b**), and a baryte crystal included in an oxide grain that forms the dark laminae in the Talat n'Ouamane sandstones (**c**). Note: The yellow crosshair marks the analysed spot.

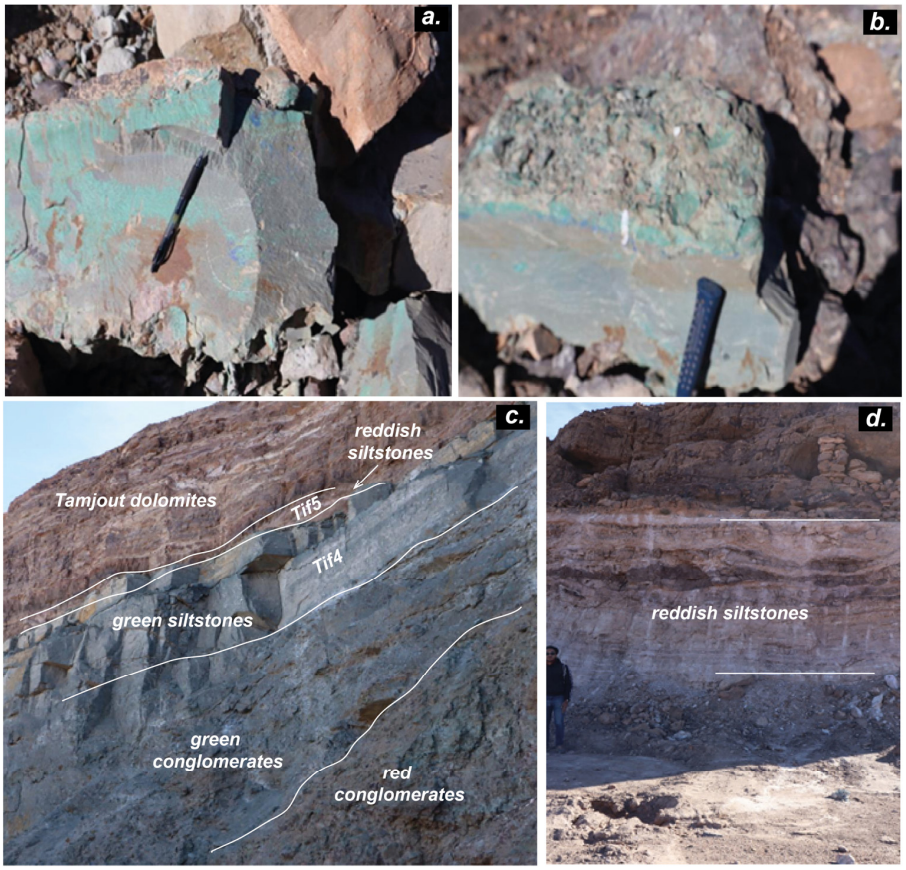



**Figure 5.** Field observation showing (**a**,**b**) malachite coatings in late fractures affecting Tif2 and Tif3 facies, (**c**) greenish to grayish non-mineralised facies (Tif4) (photo is about 30 m across), and (**d**) reddish mineralised facies (Tif5).

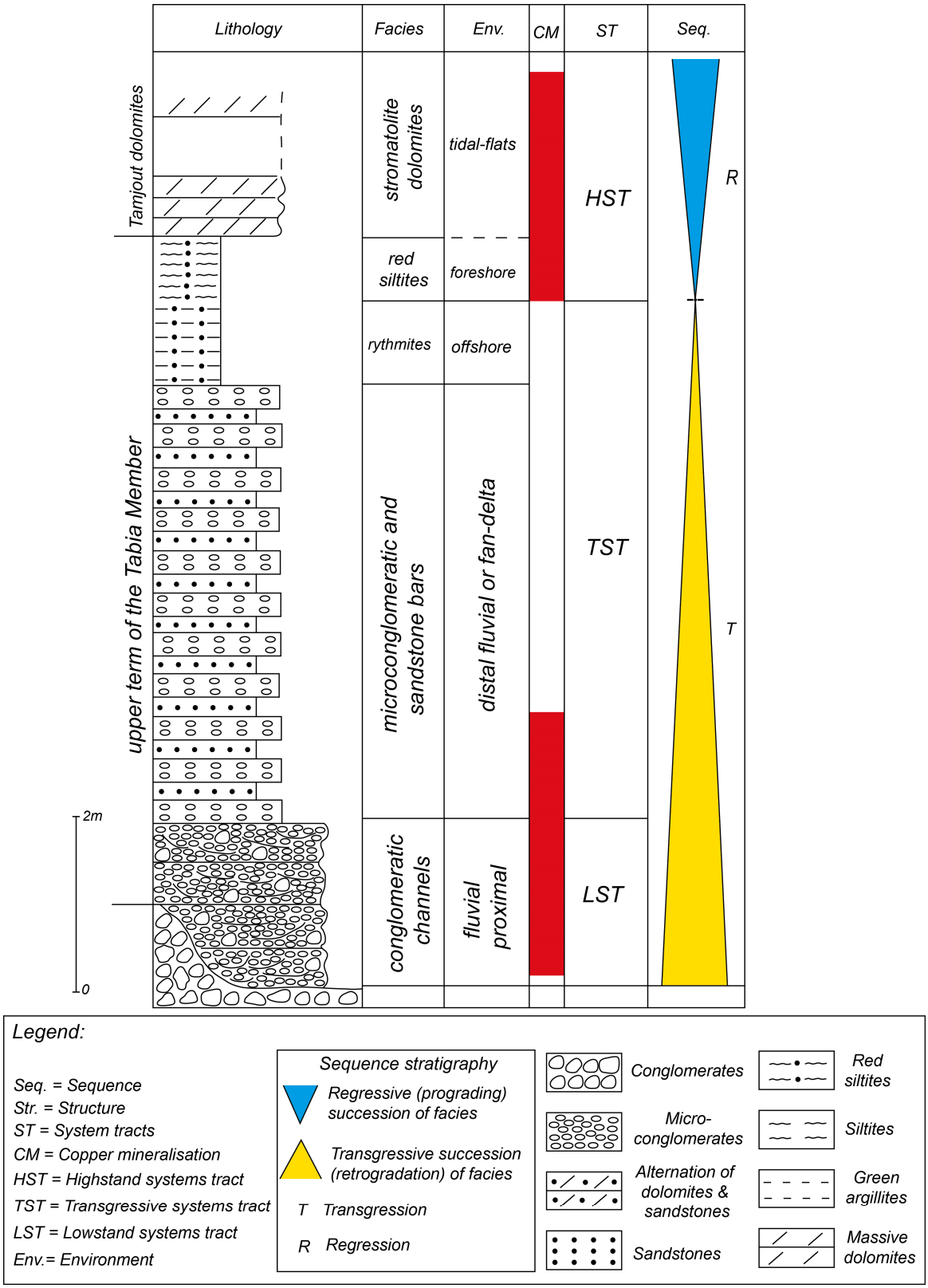



**Figure 6.** Stratigraphical log of the Tabia Member succession in the Tiferki region. The legend is shown applies to Figures 8, 10, 11, 14, 16 and 17.

In the second sequence, the horizontal geometry of the microconglomeratic beds, each capped by medium-to-coarse sandstone, and the absence of basal channelisation suggest deposition by highly concentrated sheet flows on a gently sloping submarine floor. This facies association (Tif2 and Tif3) indicates a deeper depositional environment relative to

the underlying facies Tif1. It is interpreted as representing the middle part of a submarine fan developed at the slope apron, overlying the proximal fan deposits in response to a relative rise in sea level. Consequently, this sequence represents a Transgressive Systems Tract (TST), composed of elementary sequences defined by the recurring association of facies Tif2 and Tif3.

In the third sequence, the fine grain size of facies Tif4 and the lack of subaerial exposure indicators point to deposition under quiet, deep-water conditions. This sequence is interpreted as the aggradational phase of a Highstand Systems Tract (HST), corresponding to the stage of maximum flooding.

The fourth sequence features fine-grained, crudely stratified deposits likely formed by sedimentation during flooding episodes on an alluvial or coastal plain. This sequence corresponds to a phase of relative subaerial exposure, where the mineralisation consists of a suite of oxides and hydroxides (goethite, hematite, and clay minerals). These oxides, interpreted as saprolites and laterites, result from supergene weathering and mineralisation [18,25] (Figure 7).

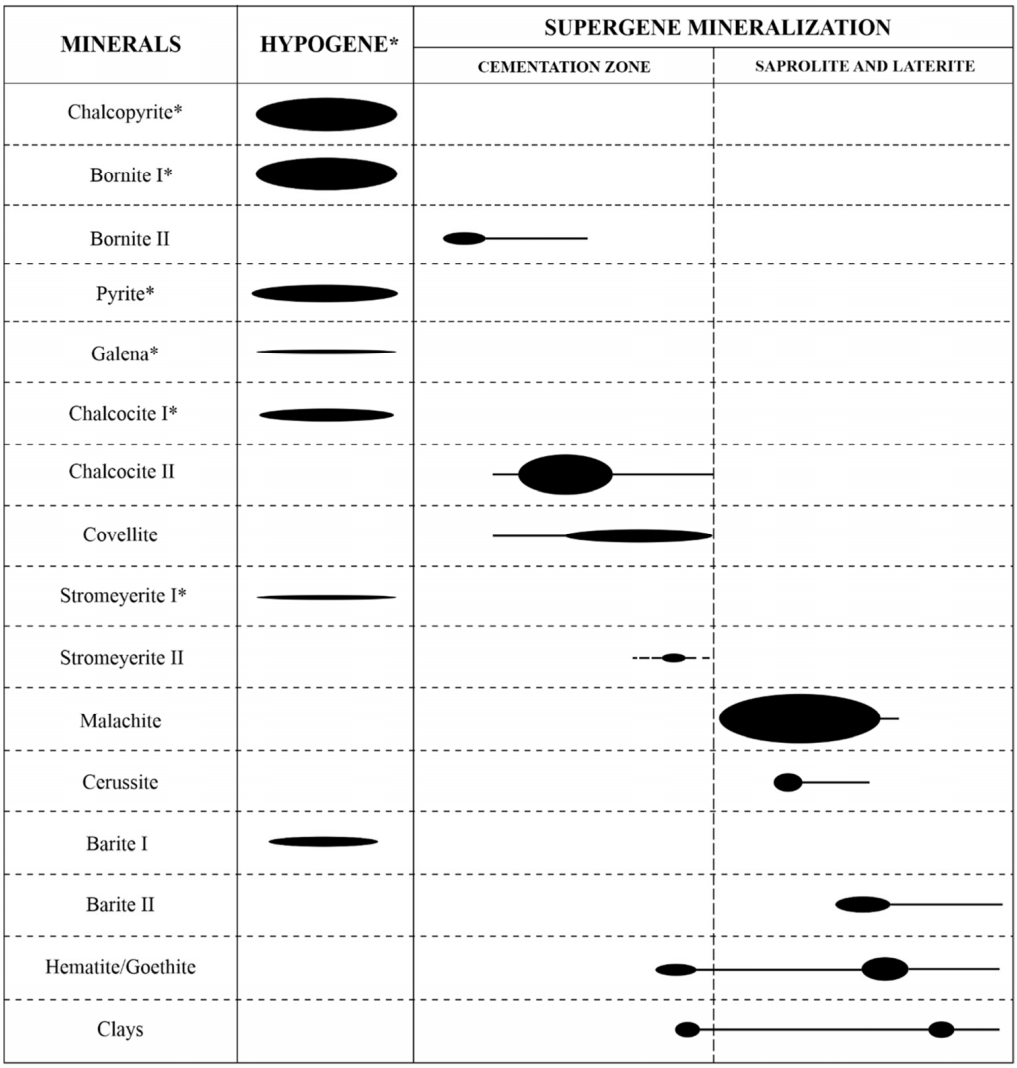



**Figure 7.** Paragenetic sequence of the Tizert deposit, showing hypogene and supergene mineralisation (after Poot et al. [25]; * observed in Oummouch et al. [18]).

### *4.2. Talat n'Ouamane Quarry*

#### 4.2.1. Description of Facies and Sequences

At Talat n'Ouamane, the sedimentary succession, comprised between the conglomerates of the Ouarzazate Group and the Cambrian Tamjout dolomites, can be subdivided into

three lithological units (Figure 8). The basal unit consists of an alternation of sandstone and micro-conglomeratic beds with purplish clay layers. The intermediate unit is a greenish clay-rich interval locally interbedded with sandstone beds, whereas the upper unit is composed of distinctly sandy bars.

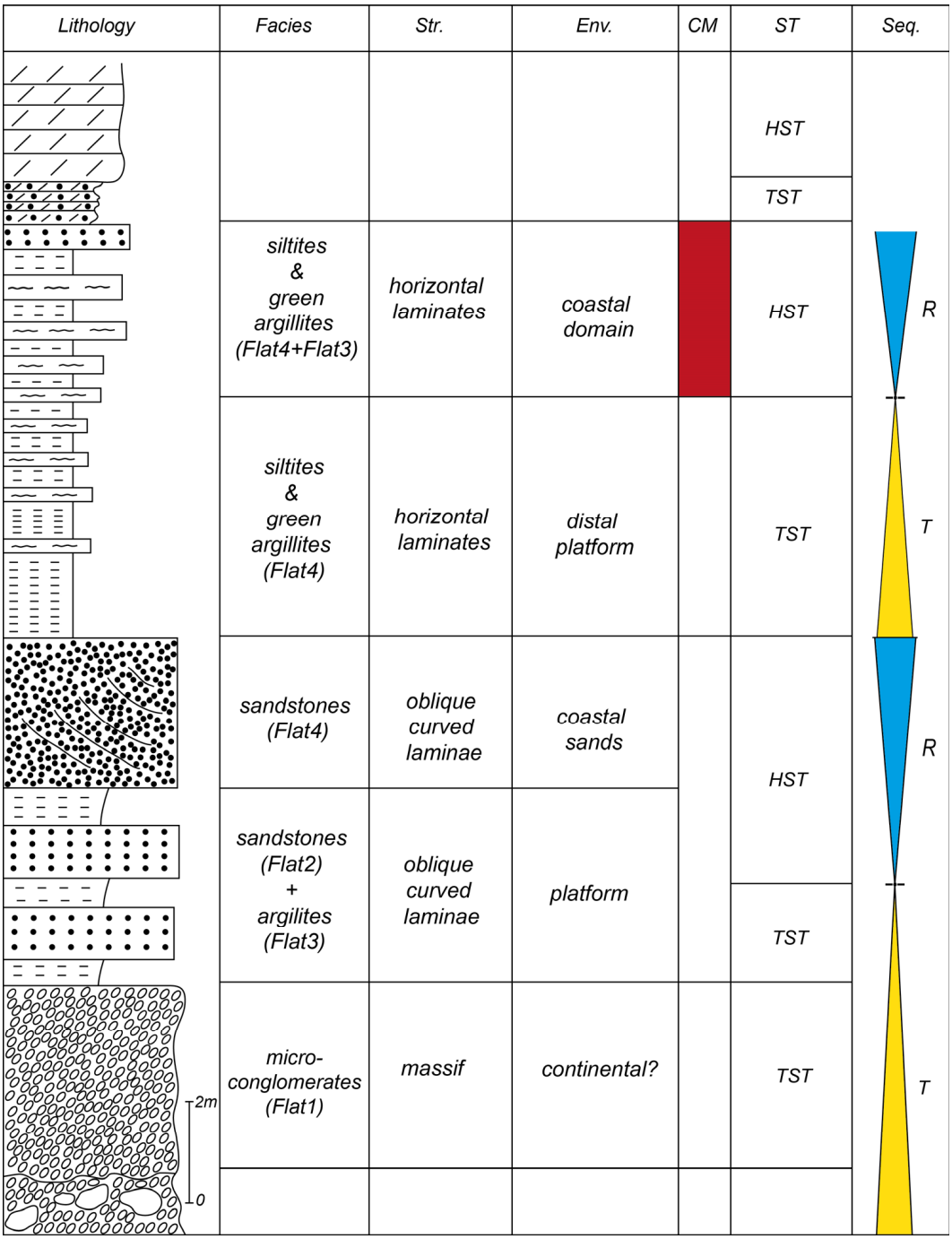



**Figure 8.** Detailed stratigraphic section of the Tabia Member at the Talat n'Ouamane region.

The basal unit is organised into four metric- to multimetric-thick sequences. The first two sequences comprise three distinct facies. The basal facies (Ftal1) consists of microconglomerate beds of variable thickness (decimetric to metric) with an erosive basal contact (Figure 9a). The middle facies (Ftal2) is composed of reddish sandstone with often oblique, arch-shaped laminations (Figure 9b), while the upper facies (Ftal3) comprise

purplish clay layers with no apparent internal structures. The two overlying sequences consist only of Ftal2 and Ftal3 facies.

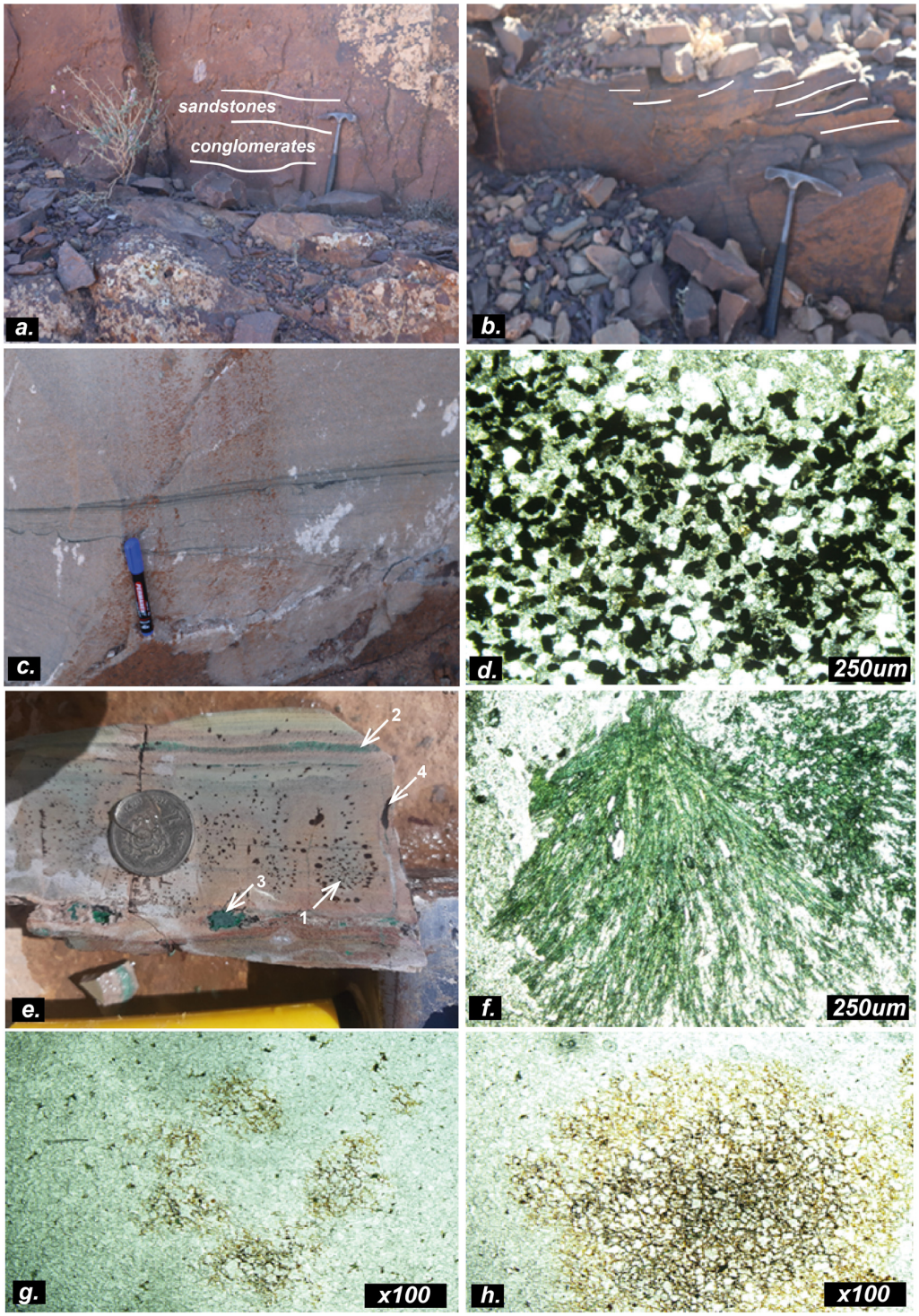



**Figure 9.** (**a**) basal micro-conglomeratic facies of Talat n'Ouamane (Ftal1), (**b**) sandstone facies with oblique laminations (Ftal2), (**c**) sandstone with slightly arched oblique laminations (Ftal4), (**d**) photomicrograph showing the oxide grains concentrated in oblique laminations, (**e**) the different aspects of copper mineralisation in fine sandstones (1—chalcocite in circular clusters, 2—sandstone layer with malachite, 3—small geode with malachite and quartz, 4—chalcocite in small cracks), (**f**) photomicrograph showing the botryoidal malachite cement, and (**g**,**h**) photomicrograph showing the circular patches of chalcocite that observed in (**e**).

The median unit is significantly thicker, approximately 14 m, and consists of alternating laminated greenish clays and sandstone beds, either massive or displaying oblique, dome-shaped laminations (Ftal4). Each sandstone–clay couple forms an elementary sequence, bounded at the base by an erosive surface.

The upper unit (~2.5 m thick), which hosts the copper mineralisation, is referred to as the "Talat n'Ouamane level" by Pouit [17]. It is composed of two sandstone bars (Tal5 facies) with internal structures exhibiting horizontal or oblique laminations, particularly at the base of the first bar (Figure 9c). These laminations contain oxide particles (Figure 9d), which a scanning electron microscope reveals to be composed of barium oxides and sulfates (Figure 5c). In addition to primary sedimentary structures, this facies displays crenulated or vertically upturned laminae, interbedded layers of soft reddish clay pebbles, and intraformational breccias. Within this prism, copper mineralisation occurs predominantly in sandstones, argillaceous–arenaceous rhythmites, and to a lesser extent, in clay and fine carbonate layers. Primary sulphides are disseminated, while oxides and copper carbonates (Figure 9e) occur in multiple forms:

- Millimeter to multi-millimeter layers rich in malachite, and rarely azurite, alternating with laminae or small unmineralised clay lenses;
- Decimeter to multi-decimeter layers of fine sandstone containing calchocite, forming circular spots from millimeters to several millimeters in diameter with diffuse outlines, often arranged in concentric patterns; chalcocite is also observed along small fissure edges as dark, elongated spots;
- Small elliptical geodes filled with quartz and copper carbonates in botryoidal cement crystals (Figure 9f);
- A greenish coating exclusively covering clay laminae surfaces and joints separating beds.

#### 4.2.2. Interpretation

In the basal unit, the vertical arrangement of facies Ftal1 and Ftal2 is typical of fluvial environments and characterises the progressive filling of small meandering channels through lateral migration within a floodplain. These four sequences may represent the continental equivalent of a marine Lowstand Systems Tract (LST) identified at Tiferki.

In the median unit, the depositional environment is interpreted as a distal platform, where normal sedimentation is represented by laminated clay facies (Ftal2). Coarse sandstone layers were intermittently deposited during storm events, as indicated by hummocky cross-stratification (HCS) structures. This unit corresponds to a Transgressive Systems Tract (TST), and the repetition of elementary sequences reflects episodic rises in relative sea level.

In the upper unit, the sandstone body directly overlies distal platform marine facies, reflecting the progradation of proximal, likely deltaic facies. It represents a Highstand Systems Tract (HST) deposited following a relative sea-level fall and is derived from continental erosion. The oxides concentrated at the base of the sandstone bar were carried as solid particles, while the copper, also of continental origin, was transported in solution.

### *4.3. Tizert Deposit*

#### 4.3.1. Tizert Section

a. Description of facies and sequences

At the Tizert mine quarry, the outcrops show detrital facies ranging from microconglomerates to clays, passing through sandstones. These facies (Figure 10) are arranged vertically to form three plurimetric sequences (Stiz1, Stiz2, and Stiz3), while the fourth sequence is of carbonate nature.

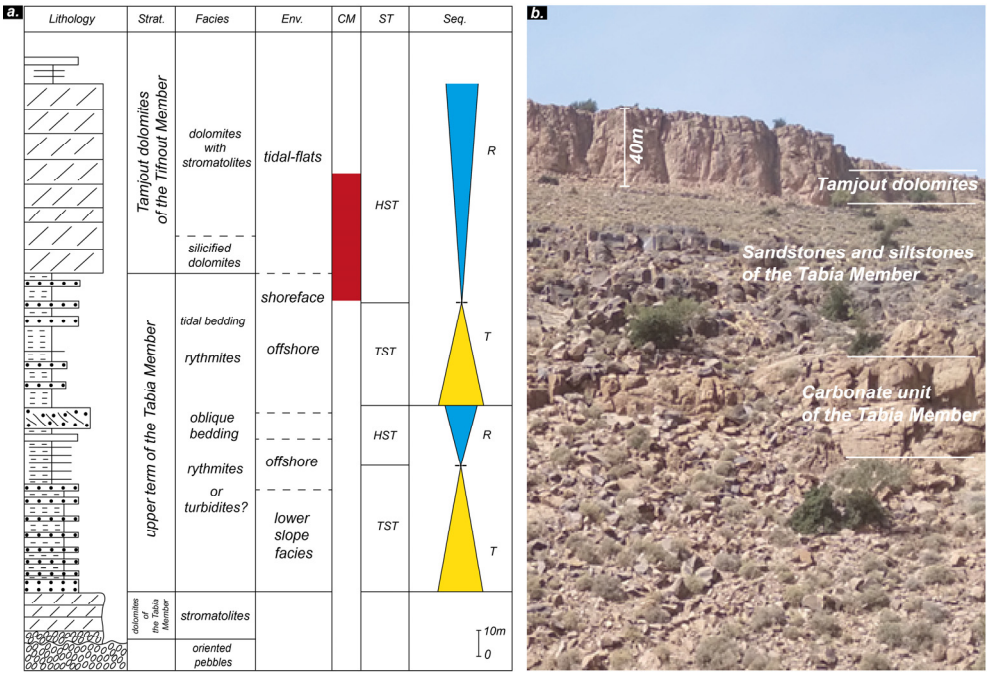



**Figure 10.** (**a**) Detailed stratigraphic section of the Tizert quarry showing the vertical succession, sedimentary structures, facies distribution, depositional environments, systems tracts (TST/HST), and sequence stratigraphy (T/R cycles) spanning from the Tabia Member to the Tamjout dolomites of the Tifnout Member. (**b**) Outcrop panoramic photograph illustrating the field exposure of the corresponding lithostratigraphic units, highlighting the distinct weathered profiles of the Carbonate unit, the sandstones and siltstones of the Tabia Member, and the prominent cliff-forming Tamjout dolomites.

The first sequence (Stiz1) rests directly on the carbonates of the Tabia Member along an erosive surface. It begins with two meters of sandstone in amalgamated beds. Each decimeter-thick bed exhibits hummocky cross-stratification (HCS) (Ftiz1) with a thin micro-conglomeratic layer at the base. This sequence ends with a metric level of black clays (Ftiz2), truncated at the top by an erosion surface.

The second sequence (Stiz3) begins with a breccia layer (Ftiz3) consisting of angular, centimetric pebbles, predominantly volcanic in origin (Figure 10). This level rests on the Stiz2 clays along an erosion contact and followed by 50 cm of black clays (Ftiz4). The sequence ends with a lenticular sandstone bar over four meters thick, showing poorly developed oblique bedding (Ftiz5 facies).

The third sequence (Stiz3), the thickest at about 20 m, allows distinction of two sedimentary corteges. The first consists of metric-scale sequences, each bounded at the base by an erosion surface. Each elementary sequence begins with a decimetric to multi-decimetric micro-conglomeratic or sandy layer (Ftiz3), and ends with decimetric to metric levels of massive or rhythmic hyperpycnites black clays (Ftiz6). The second sedimentary sequence consists of multimeter-thick clay layers intercalated with a few centimeter- to decimeter-thick hummocky cross-stratified (HCS) sandstone beds. The third sedimentary procession is represented by a single lenticular sandstone bar (maximum thickness about four meters) with large-scale oblique laminations (Figure 10).

The fourth sequence is dominated by carbonate facies. It begins with reddish clays containing a few centimetric dolomite beds, sometimes silicified, and ends with a strongly silicified (Figure 10) and mineralised carbonate ledge (Figure 10).

b. Interpretation

In the first sequence, the storm-built facies, deposited in a probably proximal offshore marine environment, correspond to a transgressive tract. The clays that overlie the sand-

stone reflect the maximum deepening, while the erosion surface indicates a sudden drop in sea level.

In the second sequence, the conglomeratic facies, generally found at the base of marine sequences, correspond to a transgressive suite followed by clay, indicating maximum deepening. The prograding stratification of the sandstones (Ftiz5) allows these facies to be interpreted as a high-level marine prism.

In the third sequence, the first elementary sequence begins with a conglomerate of the transgressive prism and ends with a rhythmic facies interpreted as a high marine level system (HST) developed during deltaic progradation, when relatively dense flows formed along the deltaic frontal slope. In the second elementary sequence, the platform facies association shows evidence of a sea-level rise, partially flooding the previously exposed platform, constituting the Transgressive Systems Tract (TST).

The fourth sequence begins with an alternation of carbonates and clays forming a transgressive prism and ends with an aggradation of carbonate facies representing the maximum depth. The carbonate nature of these facies is likely the result of climatic warming.

#### 4.3.2. Tiz C459 Borehole

a. Description of facies and sequences

This borehole begins with 36 m of micro-conglomerates (Figure 11) which is topped by a thin clay layer (about ten centimeters). Above these clays lie gray-coloured sandstones exceeding 60 m in thickness. The internal mass shows an alternation of massive, often coarse sandstone and fine sandstone layers exhibiting either horizontal planar laminations or oblique planar laminations, very rich in copper, mainly chalcocite. A notable feature of this facies is that the internal bedding is remarkably structured into bundles of fine planar laminae that systematically alternate with thicker laminae (Figure 12a,b). Outside the veins, the copper mineralisation is in perfect concordance with the sandstone laminae, whether horizontal or oblique. Another notable feature is that the size of the copper mineralisation increases proportionally with the size of the clastic particles (Figure 12c,d). When the sediment grain size becomes finer, the mineralisation appears as chalcocite spots often, organised into circular or elliptical clusters, while malachite occupies small, irregularly shaped vacuoles (Figure 12e–g).

This mineralised detrital complex vertically transitions into equally mineralised carbonates over a 4 m thick interval. This transition occurs gradually through an alternation of clays and dolomites with a characteristic reddish hue.

b. Interpretation

The thick basal micro-conglomerate unit represents transgressive prism, followed by a thin clay layer that marks a phase of maximum flooding. In the uppermost sandstone complex, horizontal or oblique planar laminae indicate a turbulent current, while the alternating bundles of thin and thick laminae reflect the periodicity of neap and spring tides. This sandstone body represents a high-level sedimentary suite. In the transition level to carbonates, the reddish colour suggests an alluvial plain environment and therefore conditions of emergence. Following this emergence, irregular cavities formed either through the karstification of the carbonates or the dissolution of evaporite crystal clusters present in the clayey–silty facies (Figure 13a–c). This emergence, probably widespread in the western Anti-Atlas, is well expressed in the Agoujgal region, where the red detrital facies contain highly oxidised mineralisation including hematite and sulfates (Figure 13d,e). It is worth noting that the very thinness of the Tabia Member at this level suggests that Agoujgal likely constituted the southern boundary of the basin during the Late Ediacaran.

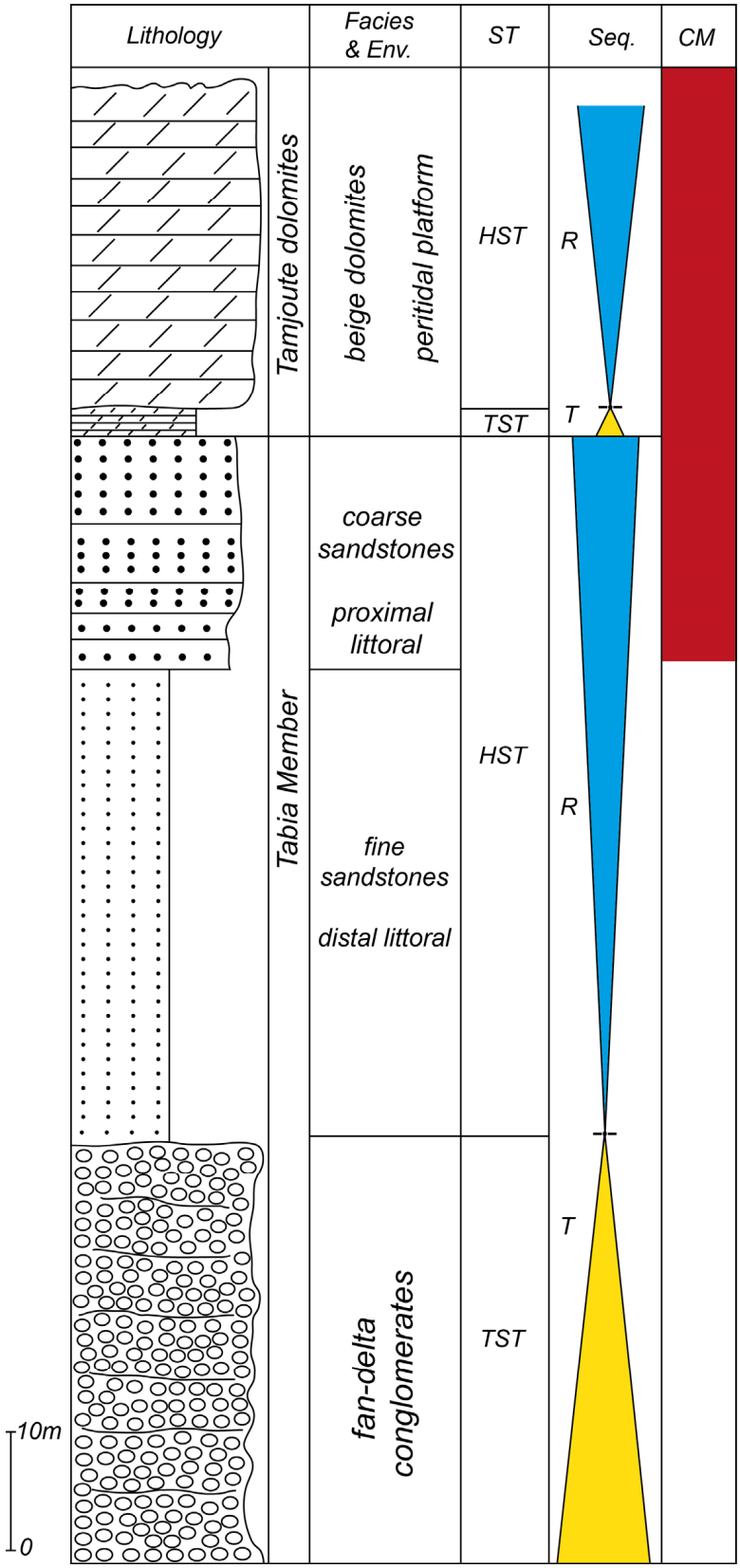



**Figure 11.** Measured section from Tiz C459 borehole showing distribution of lithofacies and stratigraphic subdivision.

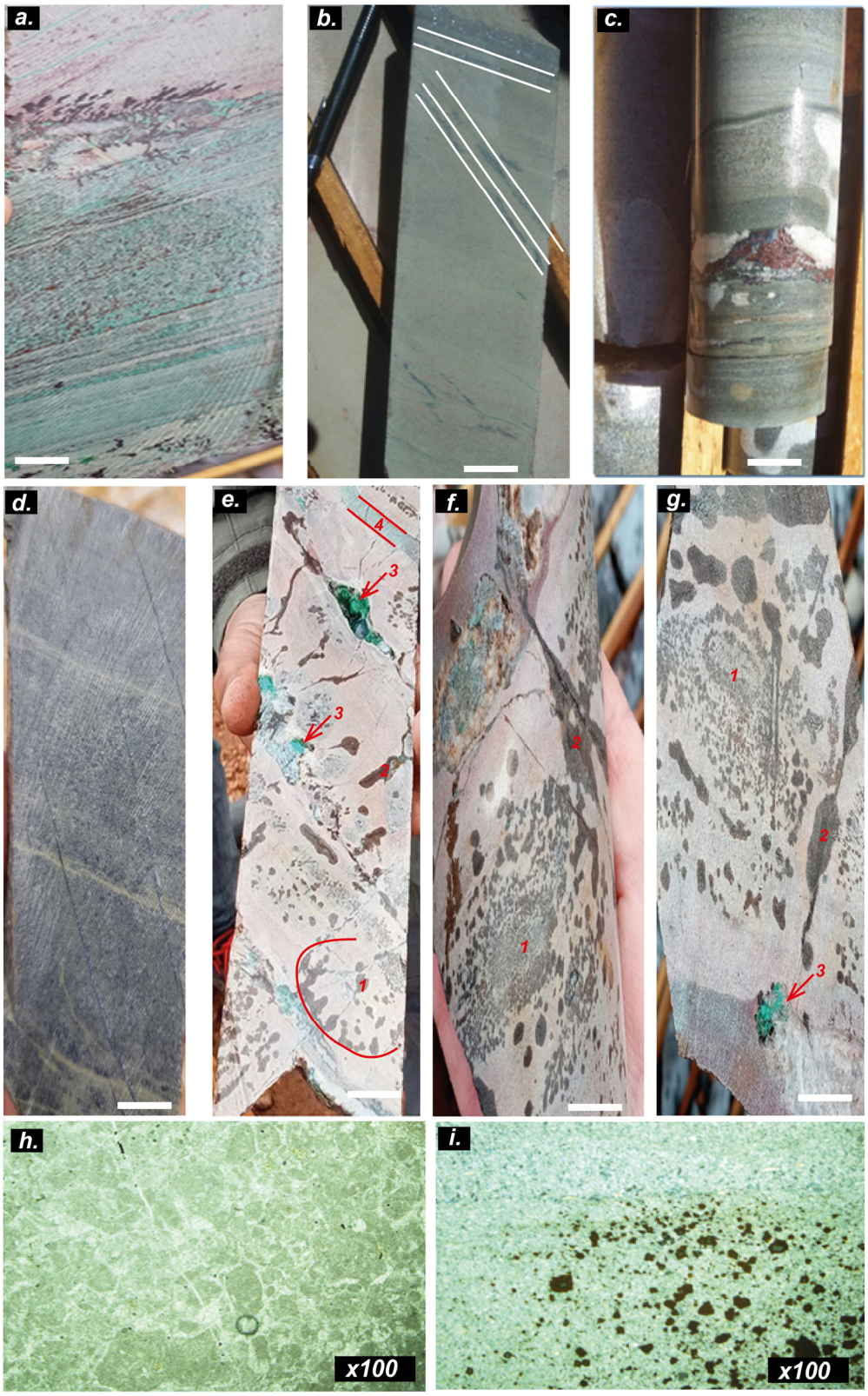



**Figure 12.** Copper mineralisation in medium sandstones concordant with horizontal planar bedding (**a**), oblique planar bedding (**b**), in coarse sandstones (**c**,**d**), chalcocite in fine sandstones in circular and elliptical masses and elongated in fissures, and malachite in small geodes (1—chalcocite in circular clusters, 2—chalcocite in fissures, 3—malachite geodes, 4—small sandstone layers with malachite) (**e**–**g**), photomicrograph showing microbes as circular spots (**h**) and selective concentration of authigenic pyrite crystals in some clay beds (**i**). Scale bars = 2 cm.

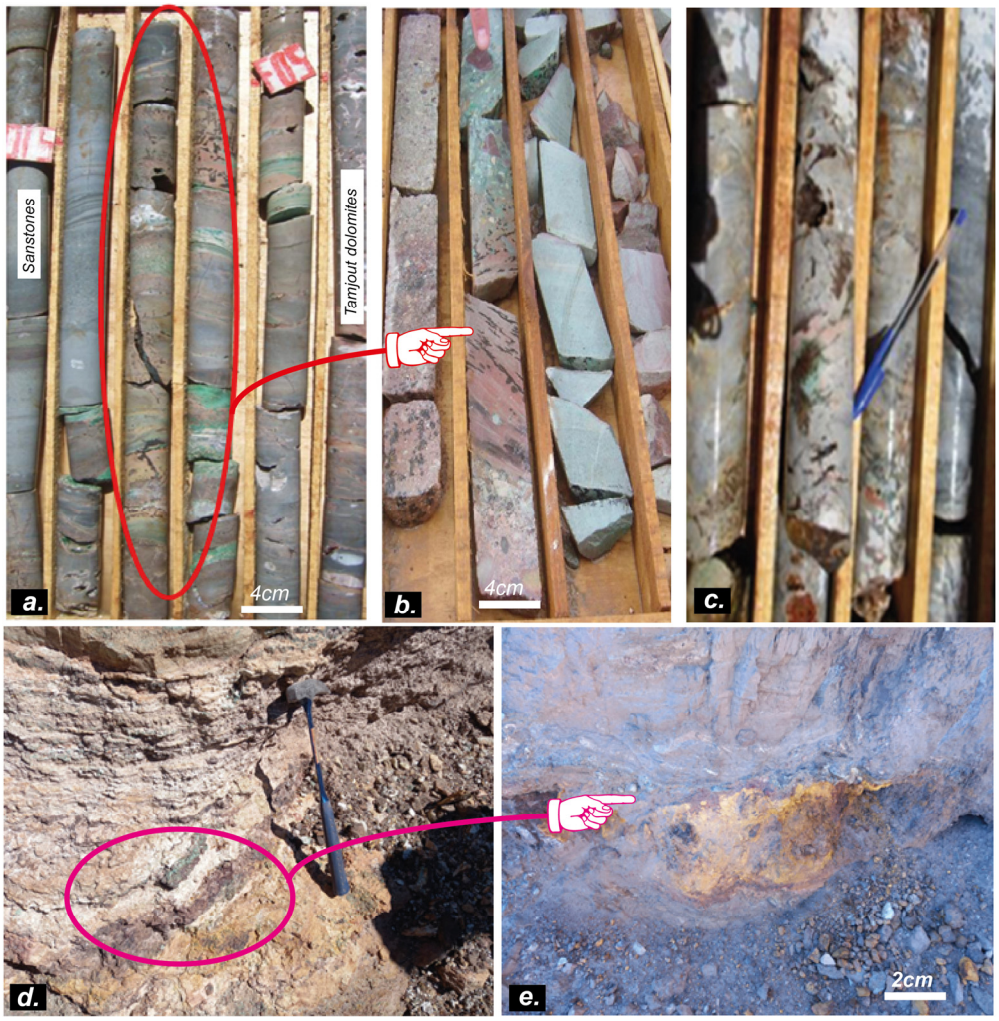



**Figure 13.** (**a**–**c**) aspect of the reddish and karstified facies of the sandstone–carbonate transition, and (**d**,**e**) oxidised mineralisation (hematite and sulfates) interstratified within the reddish emersion facies.

#### 4.3.3. Tiz C237 Borehole

a. Description of facies and sequences

The lithological succession reconstructed from the Tiz C237 borehole cores consists of three lithological units (Figure 14). The first unit exhibits an alternation of micro-conglomeratic beds, ranging from decimetric to multimetric thickness, and gray sandstone interbeds. The transition from conglomerates to sandstones is gradual, while the basal limit of the conglomeratic beds is sharp and erosive. The second unit is a sandstone complex, which is 12 m thick; its internal mass shows a millimeter-to-centimeter alternation of sandstone laminae and siltstones. The third unit (~15 m thick) is represented by micro-conglomerates in decimetric to multi-decimetric beds that alternate with sandstone layers of similar thickness. The maximum copper mineralisation is located in this unit and is expressed either by an association of bornite and chalcocite (Figure 15a) or by chalcocite and chalcopyrite, also disseminated in the matrix binding the quartzite pebbles (Figure 15b,c). The second unit is composed of a 10 m thick laminated sandstone bar covered by a 5 m thick conglomerate bar. The contact between these two facies is erosive.

b. Interpretation

The non-jointed texture of the clasts in the basal conglomeratic unit is a characteristic of debris flows. However, as in Tiferki, it can also represent a pseudo-matrix resulting from the alteration in fragile granite and quartz diorite pebbles. This suggests deposition either

in a meandering fluvial environment or at the base of a subaqueous slope. In both cases, it constitutes a low sea-level sequence.

The laminated sandstone of the second unit suggests a rise in sea level and the establishment of the initial stages of a high-level marine sequence, as evidenced by the aggrading laminae of the constitutive facies. The return of the conglomerates (third unit) records the persistence of the sea level drop, which is reinforced by an acceleration in its rate. The acceleration of the sea-level fall is clearly visible in the cover that borders the Kerdous inlier, where it is manifested by valleys incised into marine clays and sandstones and filled with micro-conglomeratic sediment shaped like an estuarine bar [32]. Progradation in all its forms testifies to the erosion of the hinterland relief, which provides both clastic particles and detrital or dissolved copper.

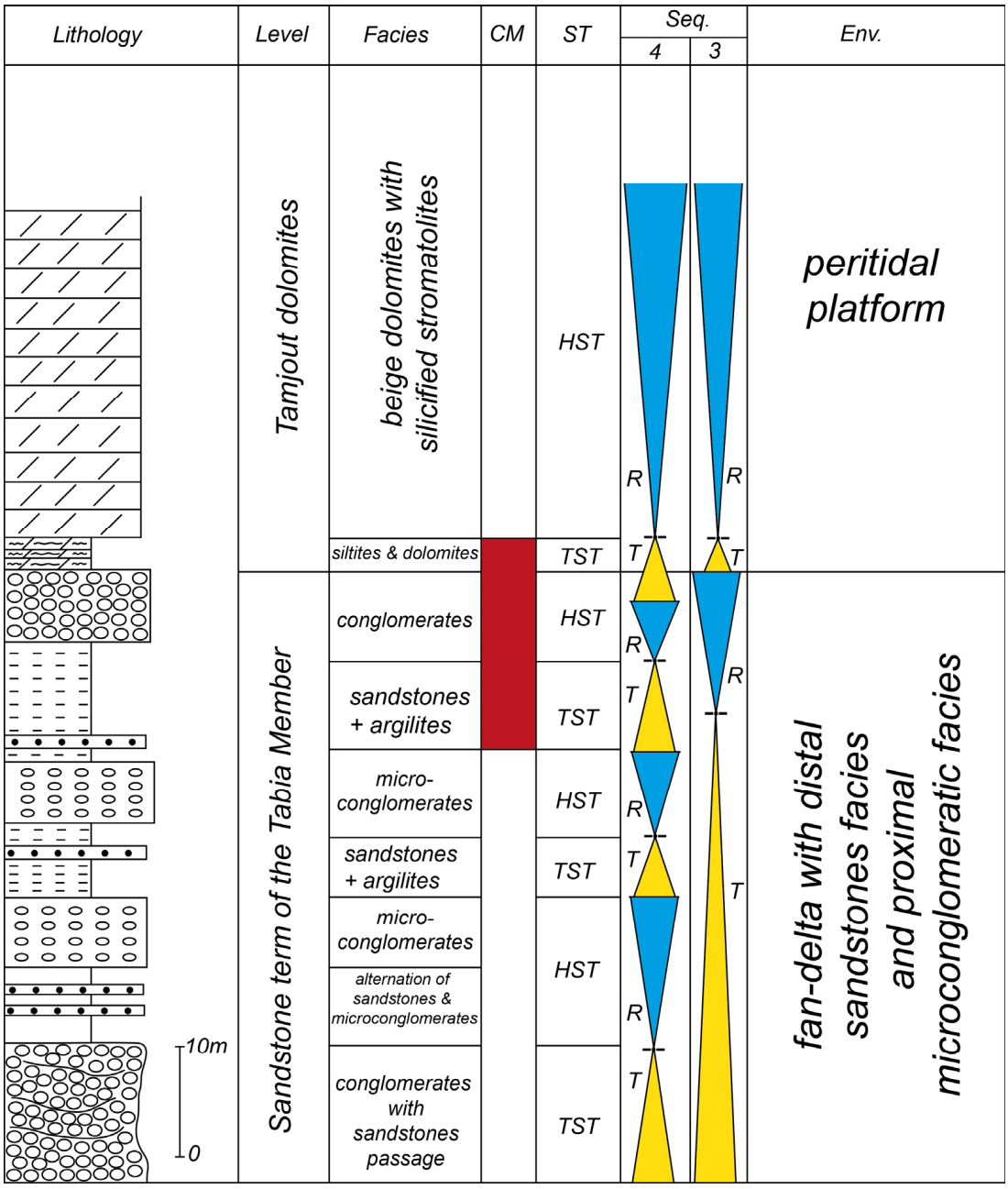



**Figure 14.** Measured section from Tiz C237 borehole.

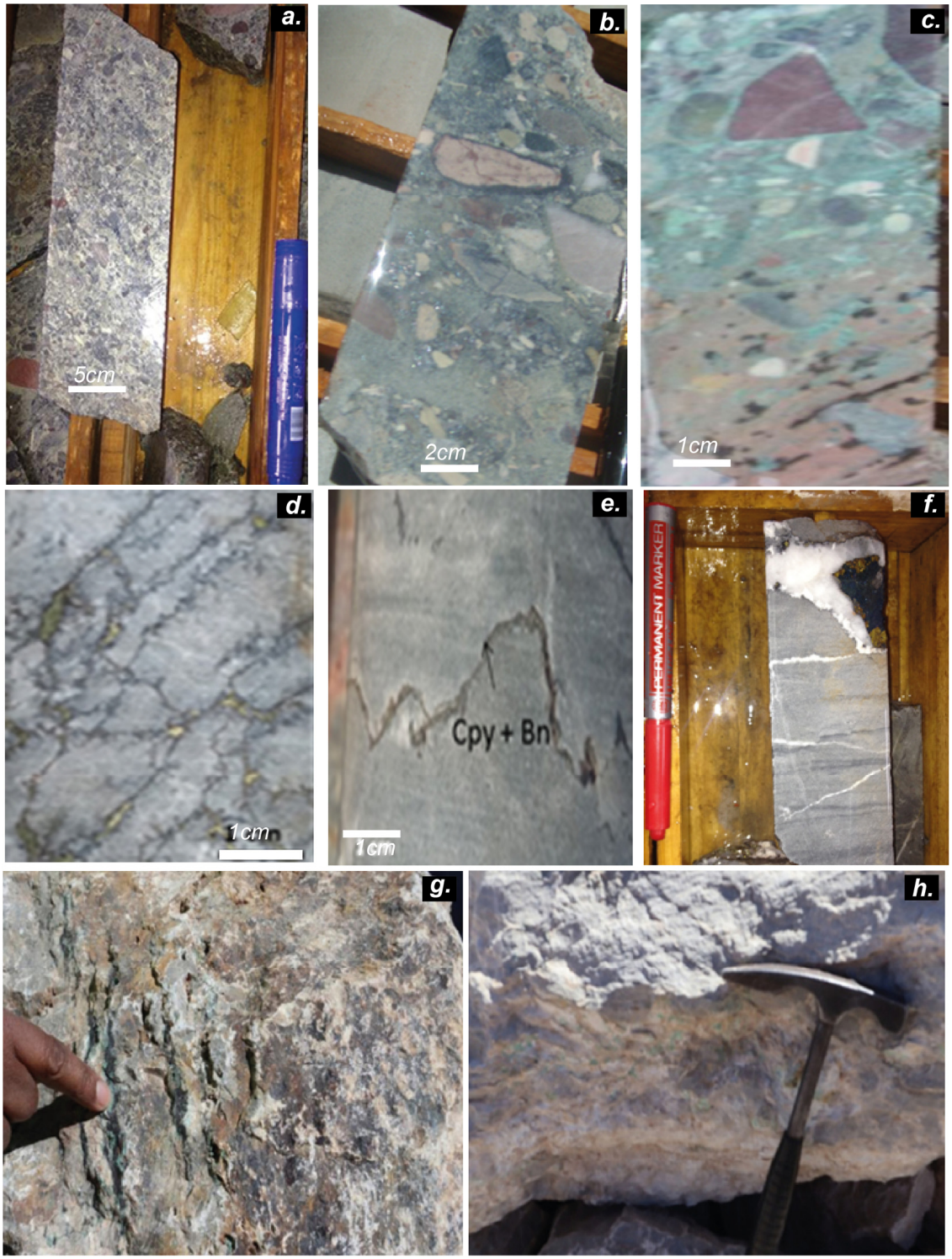



**Figure 15.** (**a**) Bornite–chalcocite disseminated in the conglomerates; (**b**) chalcocite in the sandstone matrix of the conglomerates; (**c**) chalcocite and malachite in the matrix of the quartzite pebble conglomerate; (**d**–**f**) chalcopyrite (Cpy) and bornite (Bn) in the carbonates at the stylolite level; (**g**,**h**) field photographs show the quartz vein horizon containing chalcopyrite and chalcocite within the Ouarmdaz carbonates.

#### 4.3.4. Tiz 208 Borehole

This borehole consists of a sequence (Figure 16) almost similar to that of the previous Tiz C237 borehole, the only difference being that the sandstone level of the median unit is less thick (~4 m). In addition to the 24 m of the upper conglomeratic unit (unit 3), a large

portion of the overlying carbonates is also mineralised (~30 m) in the form of chalcopyrite and bornite, which appear in quartz veins and along stylolites that affect the carbonate mass (Figure 15d–f).

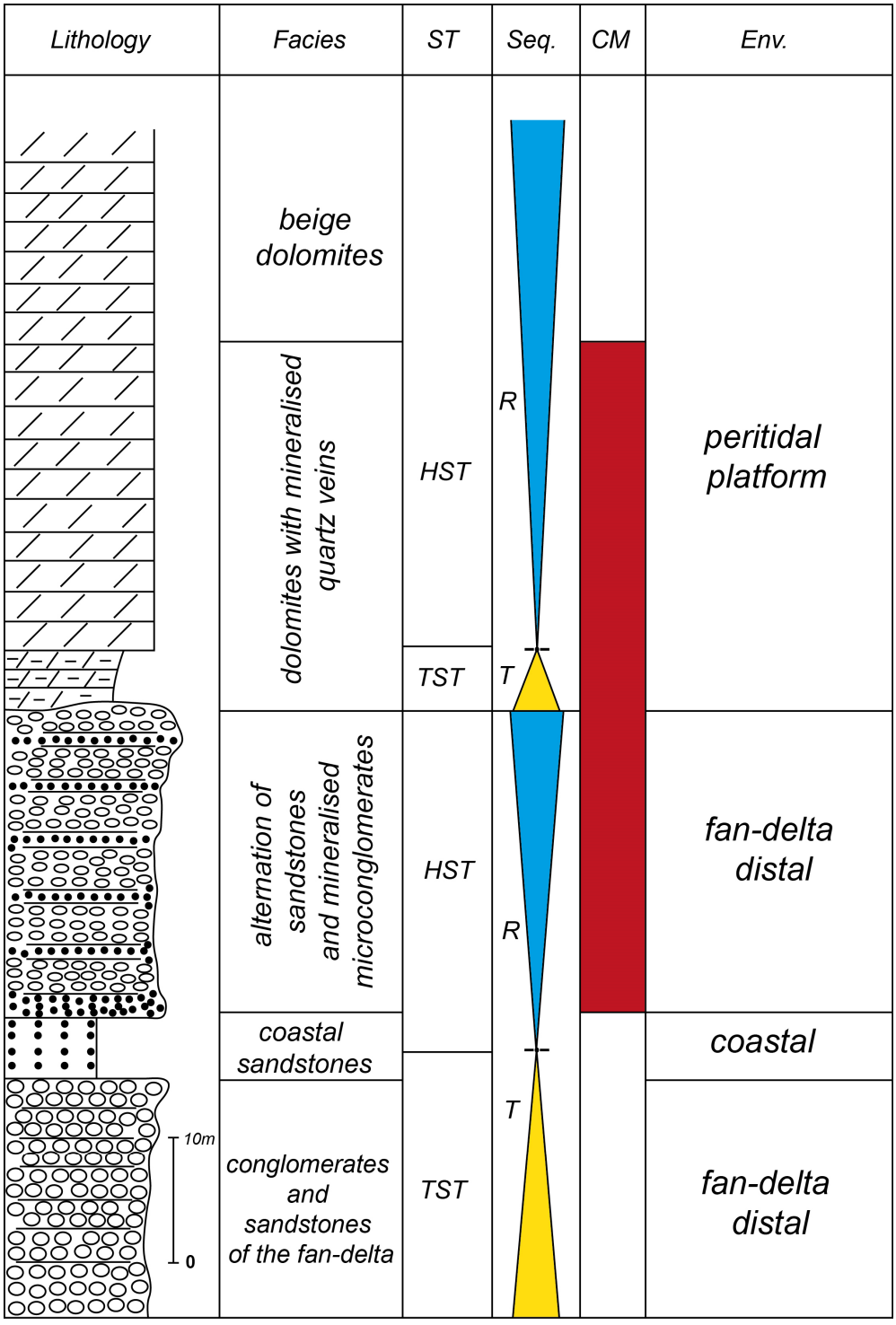



**Figure 16.** Stratigraphic section illustrating depositional systems of the Tiz 208 borehole.

### *4.4. Ouarmdaz Deposit*

#### 4.4.1. Description of Facies and Sequences

This sedimentary succession (Figure 17) is about thirty meters thick. It begins with 10 m of coarse sandstones rich in micas that rest on a conglomeratic complex with large blocks and ends with siltstones and greenish fine sandstones just below the Tamjout

dolomites. The latter, and particularly its silicified levels, constitute the most mineralised part of this deposit (Figure 15g,h).

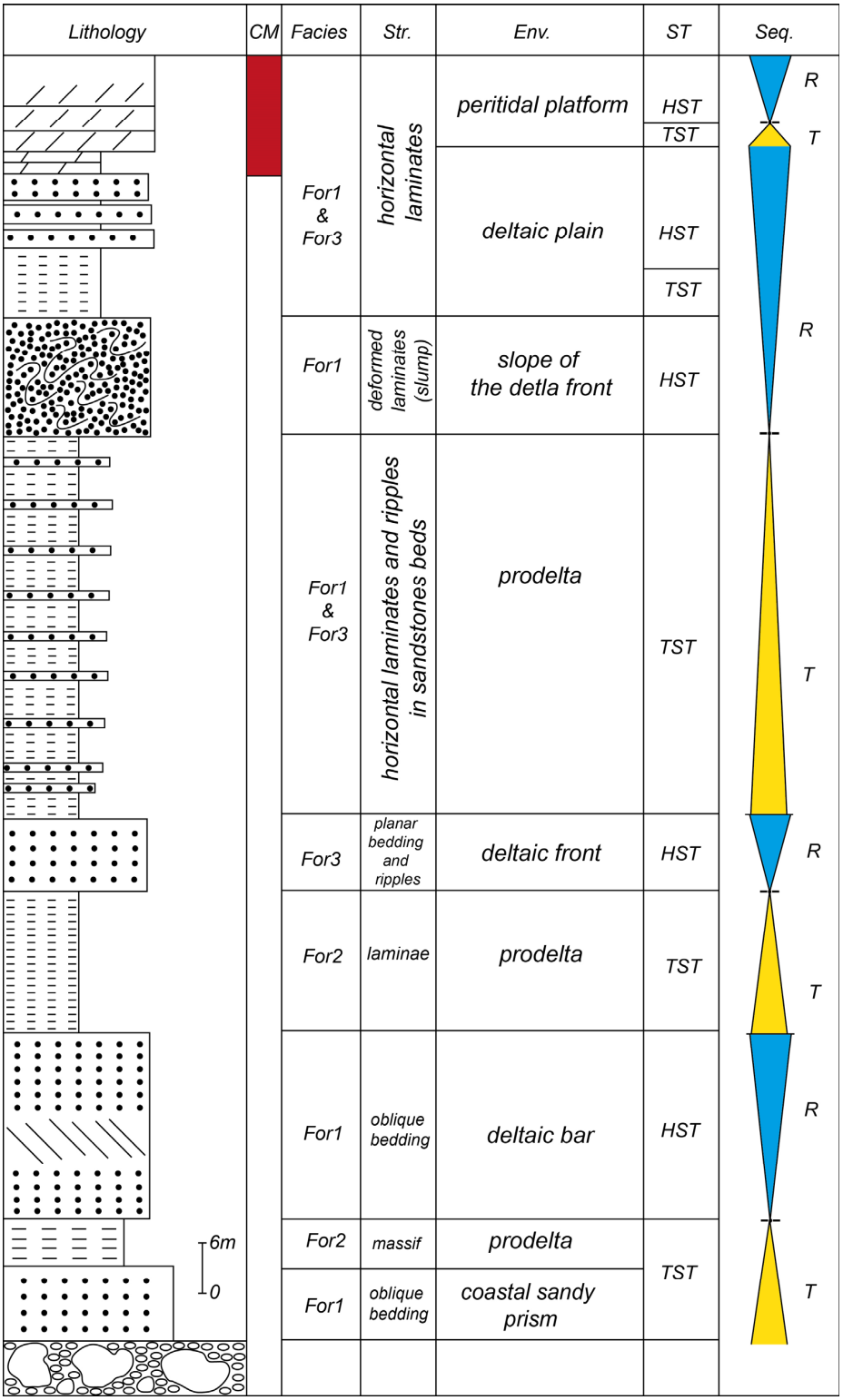



**Figure 17.** Sedimentology and stratigraphy of the Ouarmdaz quarry (Tabia Member).

The silty-sandstone term that corresponds to the TOL can be subdivided into three lithological units (Figure 17):

- The basal unit rests directly on the Neoproterozoic conglomerates via a planar contact. It consists of multimetric lenticular sandstone bars amalgamated or separated by thin

clay lenses (For1 facies). These sandstone bars gradually become enriched with clayey levels (For2 facies) and often exhibit metric-scale sigmoidal oblique laminations. This facies gradually transitions upwards to prodeltaic clays (For2).

- The median unit (approximately 15 m thick) consists of multimetric clayey–silty layers of purplish colour. The lower half of this unit is exclusively clayey, while its upper part shows intercalations of sandstone lenses (For1) whose thickness increases from decimetric at the base to metric at the top.
- The upper unit, approximately two meters thick, is represented by greenish-coloured siltstones and fine sandstones, shaped into a millimeter-scale alternation of fine laminae and relatively coarser ones. This unit, with a rhythmic distribution and no sign of emergence, is characterised by low copper mineralisation.

The Tamjout dolomites, which host the copper mineralisation, in turn show two sedimentary sequences. The basal transgressive sequence consists either of finely laminated micritic facies or of an alternation in chert layers and carbonate interlayers with storm structures (HCS). The second sequence consists of dolomitic banks amalgamated with silicified stromatolites.

#### 4.4.2. Interpretation

This basal unit, which rests on a clear planar contact with the conglomerates, can be as an advance of retrograding coastal sand prisms onto the continental conglomerates under the control of a rise in relative sea level. The strata decrease in the sandstone levels and the progressive increase in the clay levels attest to this retrogressive trend and thus the establishment of a transgressive interval (Transgressive Systems Tract, TST).

In the median unit, the basal clay facies indicates brutal deepening, while the upward-thickening and upward-coarsening of second facies characterises a deltaic complex whose two constituent elements correspond respectively to a prodelta (clays) overlain by a deltaic front in a progradational trend. This unit, therefore, represents a high-level marine prism in relation to a drop in relative sea level. In the sandstone layers, the laminae locally show structures of synsedimentary soft-sediment deformation (SSSD). By its rhythmic aspect and the absence of signs of emergence, the upper unit can be interpreted as an offshore marine deposit.

In the Tamjout dolomites, the basal transgressive sequence consists either of finely laminated micritic facies from the subtidal zone or of an alternation of chert layers and carbonate interlayers with storm structures (HCS) from the platform. The second high sea-level sequence consists of dolomitic banks amalgamated with silicified stromatolites.

### *4.5. Late Sedimentary Structures and Their Genetic Significance*

#### 4.5.1. Description

In the summit siltstone–sandstone term of the Tabia Member of the Western Anti-Atlas, the facies are generally rhythmic with clayey laminae that alternate with their sandstone counterparts. Vertically, the clay laminae become increasingly rare in favour of pure sandstone facies. Several soft-sediment structures are identified in the siltstone–sandstone facies of the Tabia Member (Figure 18a–d).

Within the carbonate facies of the Tamjout level, the evidence of this event is well recorded in the fine and impermeable micritic sediments of the subtidal zone and is manifested by a clear disruption of the internal laminae, which are either bypassed or straightened vertically (Figure 19a). The same is true for the composite platform facies, which is either brecciated (Figure 19b) or deformed in the form of carbonate sediment injections into silicified sediments (Figure 19c,d). In the intertidal to supratidal stromatolitic facies, there is no evidence of soft-sediment related to synsedimentary deformation.

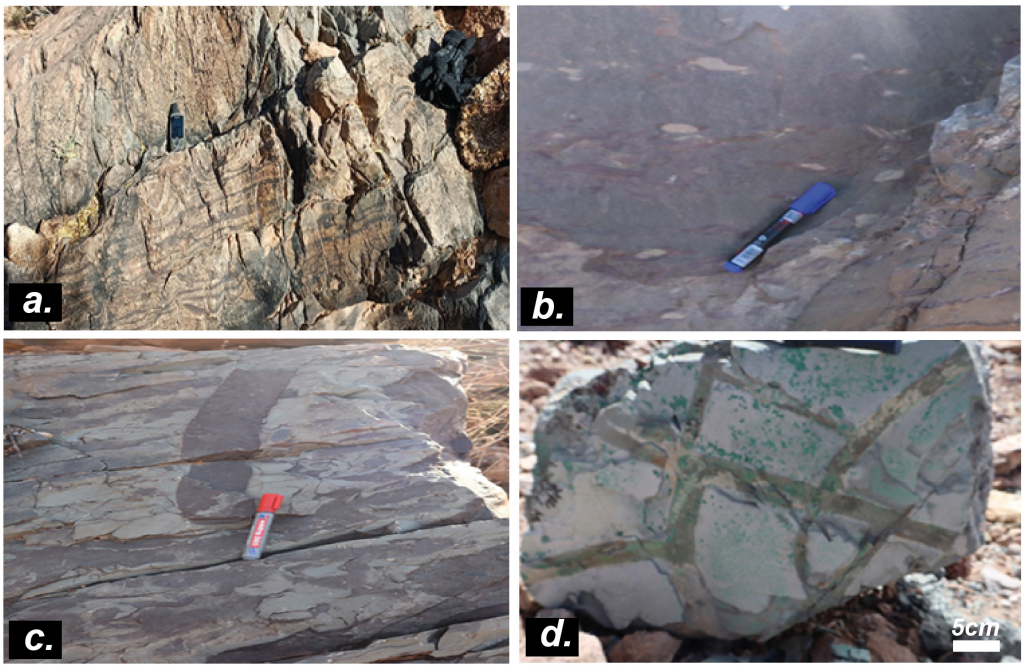



**Figure 18.** Soft-deformation structures in sandstones: induced by water escape in the form of a cupola (**a**), brecciation of clayey levels (**b**), and induced by the intrusion of liquefied sandstones into clays in the form of simple (**c**) or polygonal (**d**) clastic dikes.

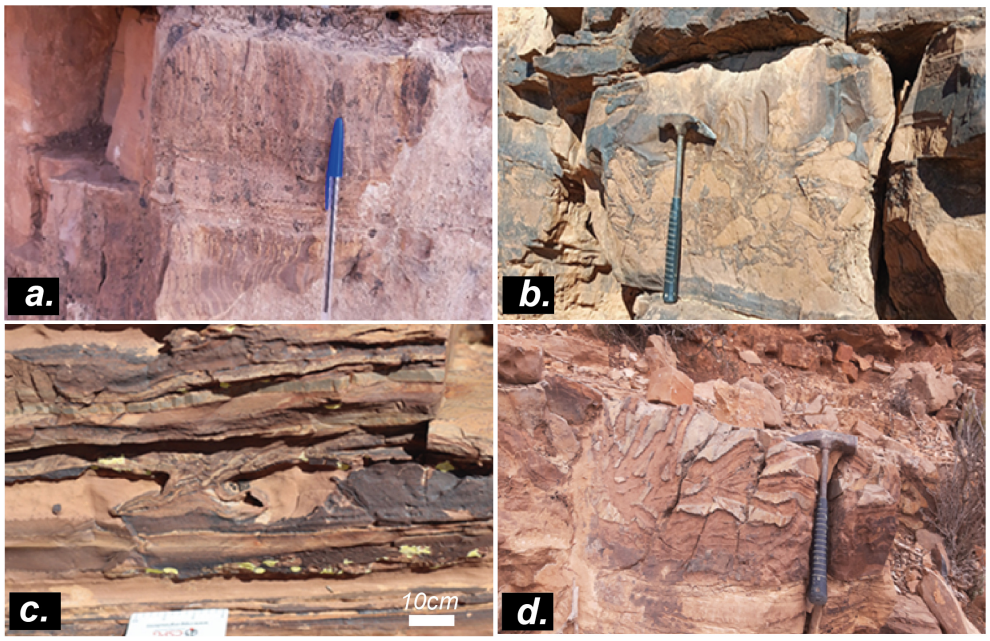



**Figure 19.** The different aspects of synsedimentary deformation in the Tamjout carbonates expressed by vertical straightening of the laminae (**a**), injection of sediment into another (**b**), load structures (**c**), and total brecciation of the carbonate–silicite alternation at the base of the Tamjout dolomites (**d**).

#### 4.5.2. Interpretation

This rhythmic aspect has allowed for a good recording of post-genetic structures where soft-sediment related to synsedimentary deformation is expressed either by the disturbance or even the brecciation of internal laminae (Figure 18a,b), or by the injection of a sandy sediment into the clays (Figure 18c,d). The flexible or brittle soft-sedimentary deformation of the internal laminae is interpreted as a consequence of water escape, while clastic intrusions are attributed to the fluidisation of a sediment and its intrusion into

the underlying layers under the effect of hydraulic pressure [48–55]. The geographical distribution over a very vast area (almost the entire territory of the Western Anti-Atlas) of these structures is evidence of the occurrence of a significant fluidisation and water escape event during the early diagenetic stage.

In subtidal carbonate facies, the fine texture of the sediments does not allow water to circulate freely, and as a result, the internal laminae of the sediment are deformed or brecciated by hydraulic pressure. Intertidal stromatolitic facies, on the other hand, are sufficiently porous and permeable to allow fluids to circulate. These porous carbonate facies would have been percolated at the diagenetic stage by acidic fluids rich in silica and copper, allowing for the karstification and mineralisation of the carbonates.

## 5. Discussion on the Origin of SSC-Type Mineralisation in the Tabia Member

In the detrital levels of the Tabia Member (siltstones, sandstones, and conglomerates), the mineralisations are primarily hosted by the sedimentary prisms of low sea level and high sea level. The transgressive or maximum deepening sequence is almost devoid of mineralisation. This selective distribution suggests that variations in relative level controlled the spatiotemporal distribution of the primary stratiform copper mineralisation of the Tabia Member. Indeed, the downward trend in sea level gradually exposes the hinterland reliefs and intensifies erosion, supplying the depositional area with detrital materials. In addition to these two episodes of mineralisation controlled by sea-level variations, a third episode related to sediment liquefaction during the diagenetic stage must have reorganised the host sediment and remobilised or even enriched the primary mineralisation. This mechanism is not limited to the Tabia Member alone but also affects the Tifnout Member (Tamjout dolomites). It is therefore possible to distinguish three stages of stratabound mineralisation in the Tabia Member. Each of these mineralisations will, in turn, be subject to remobilisation under the effect of subsequent geodynamic events that affect the region throughout its geological history.

### *5.1. First Mineralising Stage*

This stage concerns the genesis of primary sulphides in the sandstones of the basal series, which is not unanimously agreed upon by authors. Despite the diverse occurrences of copper mineralisation in the Tabia Member of Tizert, Oummouch et al. [18] suggest a single mineralising event for both the stratiform and fracture-like varieties. This mineralisation would be due to a relatively late diagenetic event with a possible syngenetic genesis of framboidal pyrite in the fine sediments. This hypothesis is essentially based on the transgressive nature of the alteration mineralisation across the different lithologies of the basal series, the absence of a stable reducing agent (organic matter), and the unavailable of a mobile reducing agent such as hydrocarbons at the syngenetic or early diagenetic stage. However, this model cannot explain the selective distribution of copper mineralisation within sedimentary assemblages, particularly at Tiferki, where the mineralised conglomerates (LST) are separated by a significant heterolithic sedimentary series lacking mineralisation (TST) from another mineralised level found at the top of the Tabia Member and in the Tamjout dolomites (HST). Furthermore, Poot et al. [25] established a clear distinction between hypogene mineralisation composed of primary sulphides and supergene mineralisation resulting from the late weathering of these primary sulphides. Figure 7 (Poot et al. [25]) indicates that the hypogene (primary) mineralisation consists of chalcopyrite, bornite I, pyrite, chalcocite I, and minor amounts of galena and barite. In contrast, the supergene (secondary) mineral assemblage is composed of chalcocite II, covellite, bornite II, malachite, cerussite, barite II, goethite, hematite, and clay minerals.

According to these authors, the weathering of the primary hypogene paragenesis gave rise to the secondary paragenesis of the supergene zone.

Moreover, the presence of a mobile reducing agent in the form of hydrocarbons is not necessarily linked to deep burial and a long formation period; biogenic methane can indeed form in the early stages of diagenesis through the decomposition of organic matter by anaerobic bacteria, a process known as methanogenesis. For our part, we believe that primary sulphides have a syngenetic or early diagenetic origin. Indeed, at the time of maximum exposure of the platform, valleys or incised channels were formed and the erosion product was largely dumped down the slope at Tiferki to form the low sea level system. The erosion of the hinterland would have brought coarse deposits derived from a basement where volcanic rocks and quartz diorites predominate. In the diorites, the very advanced alteration in feldspars into micas, as well as the abundance of authigenic ilmenite crystals in the interstices (Figure 4a) and cutting across the feldspars (Figure 4b,c), indicate that these rocks probably underwent, before their erosion, a significant hydrothermal event. In addition to the alluvium, the current would have transported detrital copper, as already mentioned by Pouit [17], and especially in solution, as suggested by Oummouch et al. [18]. It should be noted that in the Alous region, not far from Tiferki, copper mineralisation has been described in the underlying conglomerates of the Ouarzazate Group in the form of disseminated copper sulphides and stockworks [56,57]. The quartz diorites, on the other hand, may have originated from nearby outcrops. Except for a few resistant pebbles, most of the dioritic material, given its highly advanced state of alteration, is easily disaggregated and forms a clayey matrix rich in chloritised micas. The alteration in the diorites would also have released sulfate crystals into the sediment, but at this stage of knowledge, it is not possible to determine whether these inherited sulphides played any role in the copper mineralisation. What is evident is that the primary mineralisation in the form of sulphides (chalcopyrite and bornite) must have undergone oxidation into chalcocite and alteration to malachite and azurite.

In Tiferki, where this mineralisation stage is poorly documented, the only available work is that of Achnin [58], who studied the mineralogy, petrography, metallogeny, and geochemistry of the Tiferki copper deposit. At the petrographic level, the basal conglomeratic body of the Tabia Member is subdivided into two facies: (i) a purplish conglomerate at the base and (ii) a greenish conglomerate at the top. The non-mineralised conglomerate is purplish in colour; it is mainly composed of quartzite pebbles. The greenish mineralised conglomerate, on the other hand, is composed of pebbles that are primarily volcanic and plutonic. The colour difference would, according to the author, result from the oxidation state of the iron, as ferric iron is responsible for the purplish colour and ferrous iron is responsible for the greenish colour. The data from this study reveal that there are two different conglomerates: (i) a purplish conglomerate with volcanic and quarzitic pebbles; and (ii) a greenish conglomerate rich in fragile pebbles such as diorites and granites that easily disintegrate through weathering to form the matrix. The greenish colour is due to the richness of the matrix in chlorite, resulting from the intense alteration in the feldspars of the quartz diorites. This conglomerate was formed following the erosion of the purplish conglomerate and other rocks, such as diorites and granites, and its deposition was accompanied by copper mineralisation of detrital and chemical origin, and this mechanism better explains the total absence of mineralisation in the purplish conglomerates at the base and the transgression facies (Tif2 and Tif3). On the metallogenic level, Achnin [58] notes the existence of primary sulphides in the form of chalcopyrite and bornite, which have undergone a series of remobilisations as evidenced by the richness of the conglomerate in malachite and azurite.

Although the syngenetic or early diagenetic mechanism we have suggested can explain the presence of primary sulphides in specific sedimentary assemblages, which the late diagenetic model cannot do, the main challenge is to explain how reducing conditions are established in the deposition environment. Some supporting arguments can be found in the geomorphological features of the basin himself. Indeed, data from the literature show that from the beginning of the formation of the Cambrian sedimentary basin, the western Anti-Atlas was a graben controlled by extensional faults [32,59]. This graben coincides with the location of a basin that Boudda et al. [60] delineated based on the geographic distribution of outcrops and the thickness of the basal series (Figure 20a). This reconstruction shows that it is a semi-enclosed basin, bordered by paleo highs to the North, South, East and even to the Southwest where it is bordered by the relief of Sidi Ifni (Benziane et al. [61], Figure 20b). To the Northwest, it probably communicated with an open sea via a shallow, semi-enclosed strait. This basin (Figure 20c) would probably be similar to that of the present-day Black Sea depression, where saline and anoxic waters prevail except at the surface where water circulation allows exchanges with the open sea. During the drop in sea level, a large part of the sediments coming from the hinterland of the basin reaches the anoxic basin, after being transported by density or hyperpycnal currents to form the distal zone of a fan-delta. These turbidite-like facies are referred to as hyperpycnites [62]. During the rise in relative sea level, the deposits become dark or greenish clays and silts, organised in an alternation of millimeter to centimeter-sized laminae. Within this alternation, some laminae are remarkably studded with euhedral pyrite crystals, while others are completely devoid of them. The selective distribution of pyrite (Figure 12i) testifies to the richness of the host laminae in organic matter. Indeed, authigenic pyrite appears during the anaerobic decomposition of organic matter during early diagenesis stage [63]. The existence of unoxidised organic matter within the clays is evidence of the reducing conditions that prevailed in the basin. Further evidence reinforcing this possibility is provided by the microbial genesis of framboidal pyrite in siltstones during the syngenetic stage [18]. The anaerobic degradation of microbial organic matter may produce a mobile reducing agent in the form of biogenic methane, allowing the genesis of primary sulphides. At the scale of the western Anti-Atlas, the basin where the Tabia Member sandstones were deposited shows a geographical zonation of facies similar to that established by Pouit [17]. Four zones can be distinguished going from East to West (Figure 20d): (i) a zone of continental conglomerates; (ii) a zone of oxidised red sandstones; (iii) a zone of greenish sandstones containing sulphides; and (iv) a clayey zone devoid or weakly mineralised.

### *5.2. Second Mineralising Stage*

Following an episode of transgression relayed by a stage of maximum deepening, the mineralisation fades before resuming with the drop in relative sea level. This change in trend would have forced the sandy sediments to prograde over the platform clays while bringing copper essentially in solution. The mechanism of mineral concentration is not easy to establish, but without excluding the possibility of a detrital copper input, it is very likely that the tide first shaped the detrital particles into thick laminae during the spring tide stage and into thin laminae during the neap tide stage. The copper in solution would then have precipitated in the form of a cement that deeply permeates the sediment while respecting the initial bedding of the facies. The more agitated the tidal current, the larger the sediment grain size and, with it, the size of the intergranular spaces that harbour the copper. Unlike the coarse-grain size, the fine sandstone sediment only shows circular, elliptical, or even elongated patches of chalcocite (Figure 12e–h). These forms are not random but reveal a construction engineering that is usually found in microbial communities that proliferate inside or on the surface of fine sediment still saturated with

water. These microorganisms indeed live in the form of clusters, clumps, discontinuous nodules that are more or less concentric, pinnacles, and pustules [64]. Examples have been reported in the Ediacaran formations in South Australia [64] and in the Proterozoic basins in India [65]. These circular and elliptical structures, known as Discoidal Microbial Colonies (DMCs), have recently been documented in the current coastal plain of the Gulf of Cambay in India [66]. DMCs and other benthic microbial forms have a great capacity to precipitate a wide variety of authigenic minerals, particularly sulphides [64,67–74]. In addition to this forced precipitation, mineralisation in the form of chalcocite appears in small fissures within the clay sediment. The mineralising solution is likely injected into these small fractures, and the sulphides precipitate there in the form of chalcocite, which diffuses slightly on either side of the fissures (Figures 9e and 12f,g). In the Tiz 208 and Tiz C237 boreholes, the mineralised facies transition to conglomeratic intervals, controlled by an accelerated fall in sea level. Chalcocite I, belonging to the hypogene stage, is interpreted by Oummouch et al. [18] and Poot et al. [25] as having precipitated within sediment pores during a syngenetic or early diagenetic phase. In contrast, chalcocite II occurs within the peripheral supergene enrichment zone of the deposit and along fractures [18,25]; according to these authors, it formed via the alteration and replacement of the associated primary sulfides (bornite and chalcopyrite). The decrease in the water column in the environment is further confirmed by the emergence recorded by the reddish facies of the alluvial plain that immediately precedes the carbonate sedimentation. The example of the Agoujgal site, where small lenses containing hematite and sulfates appear within the ochre siltstones and clays, clearly confirms this emergence. The reddish facies, as well as the stratiform mineralisation dominated by oxides, are characteristic of "Red Beds" type deposits. They testify here to the syngenetic origin of the primary stratiform sulphides of the Tabia Member. These sulphides will obviously undergo remobilisations and alterations depending on subsequent geodynamic events.

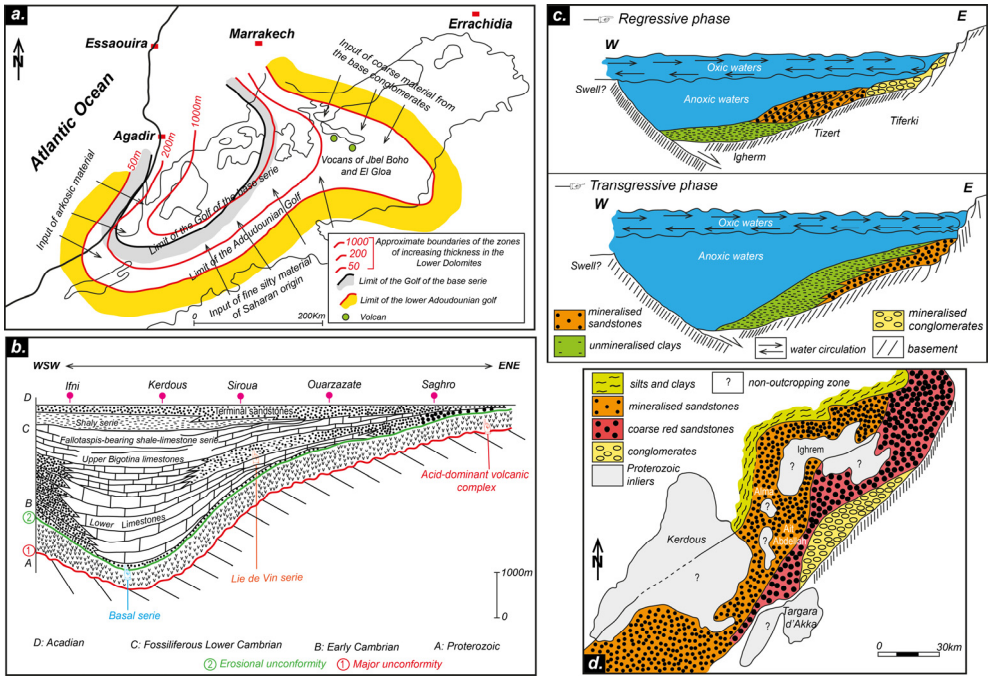



**Figure 20.** (**a**) Geographical limit of the basin during the deposition of the Tabia Member (modified from Boudda et al. [60]), (**b**) shape of the Cambrian basin according to Benziane et al. [61], and (**c**,**d**) reconstruction of the basin shape and the hydrodynamic conditions necessary for the emplacement of the stratiform copper mineralisation of the Tabia Member.

### *5.3. Third Mineralising Stage*

The abundance of mechanical structures related to water escape in the silty–sandy facies of the Tabia Member suggests extensive post-sedimentary percolation of the sediment by waters rising from depth, escaping vertically under pressure. This fluid movement is capable of significantly liquefying sandy layers, particularly those interbedded with clays (Figure 9e). The influx of water into the permeable sandstone allows copper to easily alter under oxidative conditions. This is probably how the secondary paragenesis (chalcocite and bornite) at the base of the Tizert stratiform body was formed; the pyrite and chalcopyrite zone is spared because it is hosted within much finer sediments. At the top, where the sediment becomes fine and laminated, the upward force of the mineralising fluids may, in the extreme case, even detach clay laminae from one another, as well as separate clay interlayers from adjacent sandstones (Figure 12f,g). These fluids can then diffuse laterally and coat impermeable surfaces with copper carbonates. When fluid is trapped in small voids created by overpressure, dissolved ions can slowly precipitate as quartz and copper carbonates with a botryoidal structure (Figure 9f). This remobilisation of copper is likely a consequence of the intense liquefaction and water escape event that generated various deformation features throughout the Western Anti-Atlas. Such liquefaction events, which must be limited in duration, can only occur through the forced injection of large volumes of water that subsequently rise under pressure as soon as they encounter an impermeable surface [55].

At the level of the Tamjout dolomites, although the typology of the copper mineralisation differs from that seen in the TOL and the Tiferki conglomerates, it may result from the percolation of carbonates by escaping waters, since the mineralisation preferentially concentrates in karstic pockets. The genetic mechanism would, nevertheless, be comparable to that induced by the upward escape of water. A powerful water jet would have deformed the laminae of the transgressive prism facies, then karstified and brecciated the stromatolitic levels that had undergone early lithification, while simultaneously silicifying the stromatolitic layers.

On a metallogenic level, the studies conducted by Poot et al. [25] focus on the altered deposit described as supergene because the host facies outcrop at the surface. Copper carbonates are dominated by malachite, while azurite is notably absent. The paragenesis of this alteration zone is represented by covellite, bornite II, and chalcocite II. This is considered the result of an alteration in primary sulphides that were originally present within the host rocks. This assumption, supported by the presence of galena in a single sample of Tamjout dolomites at the Issedrin site, suggests the destruction of primary sulphides on site.

This highly advanced alteration process can only occur under specific conditions: (i) the presence of acidic fluids capable of leaching primary sulphides; (ii) an oxidising environment; (iii) porous and permeable host rocks; (iv) tectonic uplift and fracturing of the parent rock to allow percolation by meteoric waters; and (v) the presence in the parent rock of a sufficiently high level of carbonates and chlorites to neutralise acidic meteoric fluids during the oxidation of primary sulphides. While these conditions are achievable in the porous carbonate substrate of Tamjout, they do not apply to the greenish clays of the upper part of the Tabia Member.

At Talat n'Ouamane, for example, these impermeable rocks are remarkably rich in malachite, which appears as thin films coating the surfaces of the clay laminae. Malachite also forms small geodes located just below certain clayey layers. These malachite occurrences in the greenish clays cannot be explained by simple diffusion of meteoric waters through the sediment, as it is not permeable. The clays are not porous enough to allow for

the occurrence of disseminated primary mineralisation that would have resulted in copper carbonates through weathering.

We hypothesise that the supergene copper deposit of Tizert was formed through per ascensum percolation of acidic waters that leached the hypogene deposit. Evidence of upward percolation is supported by the sedimentary structures observed in the Tabia and Tifnout members; however, the origin of the large volumes of water injected across a vast territory remains less clear. It may involve forced injection of water followed by its subsequent rise to the surface, a circulation mode well-documented in both ancient and current glacial environments [75,76], as well as in basins bordered by large orogenic chains undergoing uplift [77].

At present, a glacial origin cannot be considered because the last Ediacaran glaciation in the Anti-Atlas occurred around 580 Ma. In contrast, the Katangan basin in Central Africa hosts a large stratiform copper belt, and since it is located at the foot of a major mountain range, heavy rainfall in the hinterland provides the source of waters that infiltrate down to deep brines before rising to the surface through the numerous faults affecting the basin [78]. While this mechanism can explain water circulation in that region, it seems inadequate for the Anti-Atlas, where the Pan-African chain has already been eroded by the Ediacaran–Cambrian transition. Furthermore, the tectonic regime in the Anti-Atlas is extensional, unlike the Katangan basin, where tectonic shortening continuously rejuvenates the relief of the hinterland.

Hayes et al. [79] suggest, by analogy with petroleum systems, that there must be an outflow of groundwater carrying the necessary mineralisation for the formation of SSC-type deposits from depth. The waters responsible for this flow would originate from a large watershed, heavily fed by rainwater infiltrating fractured rocks. As these waters rise, they must pass through source rocks before reaching the surrounding rocks. Migration paths could include normal faults in the Kupferschiefer in Poland [80] or simply crossing coarse sediments from the basin margin [79]. The proposed mechanism for the Anti-Atlas is the vertical crossing of sedimentary layers by water, where conglomeratic and sandstone rocks are permeable, while clays show evidence of synsedimentary soft-sediment deformation (SSSD) that would allow the passage of vertical water jets.

The compilation of these data demonstrates the existence of at least three levels of stratiform copper within the Igherm district. The two well-known and more widely exploited ones are: (i) the hypogene deposit, composed of primary sulphides hosted the sandstones of the Tabia Member [18,25]; and (ii) the supergene deposit, consisting mainly of copper carbonates hosted by the upper clays of the Tabia Member and the Tamjout carbonates [25]. The third level is represented by the basal conglomerates, where copper occurs as both primary sulphides and copper carbonates. This third deposit is only present at Tiferki, where it lies directly on an erosional contact above the Ouarzazate Group, which consists of sterile, coarse-pebble red conglomerates. Furthermore, it is separated from the overlying Talat n' Ouamane deposit by a complex of non-mineralised, green laminated siltstones, interpreted as a Transgressive Systems Tract or a maximum flooding interval.

At Tizert, the boreholes examined, as well as those studied by other authors (e.g., Oummouch et al. [18]), may never have reached the contact between the Tabia Member (basal series) and the Ouarzazate Group (generally volcano-detrital). Indeed, the transition between these lithological units is marked in outcrop (Figure 10) by a carbonate level several meters thick. Generally, this carbonate unit, which constitutes the middle part of the Tabia Member, rests either on the basal conglomerates of the Tabia Member or directly on the Ouarzazate Group deposits. The Tizert boreholes have never provided evidence suggesting the existence of this marker layer (carbonates), as they are consistently terminated upon reaching the first conglomeratic or micro-conglomeratic facies, even in the absence of an

erosional unconformity like that seen at Tiferki. Consequently, available borehole data do not allow us to determine whether a conglomeratic deposit to that of Tiferki exists at Tizert.

## 6. Conclusions

The stratiform copper mineralisation of the Tabia Member, hosted within detrital sediments, corresponds to an SSC-type deposit (sediment-hosted stratabound copper). Field observations indicate that the establishment of these mineralisations coincides with the only stages of sea-level fall, whereas transgressive phases and maximum flooding appear unfavourable for copper mineralisation.

At Tiferki, for example, mineralisation occurs within a conglomeratic complex associated with maximum sea-level fall. The sedimentary material derived from continental erosion was likely enriched in copper, both in solution and possibly in detrital form, and was deposited along basin margins where reducing conditions favoured the precipitation of copper, initially as sulphides that were later altered. The equivalent of this deposit may not exist in Tizert or has simply not been reached by drilling.

Within the silty–sandy complex corresponding to highstand sedimentary sequences, continent-derived sediments form a prograding coastal prism. In this setting, copper sulphides precipitated in a tidal-dominated coastal environment as well as in a subtidal environment strongly influenced by microbial activity. The subsequent drop in sea level ultimately led to subaerial exposure immediately prior to the onset of Cambrian carbonate sedimentation. These conditions promoted the oxidation of the mineralisation and the formation of "Red Beds", providing additional evidence for the syngenetic nature of the stratiform copper mineralisation in the Tabia Member.

The sulphides were subsequently remobilised during a significant fluidisation event that deformed the host facies, leading to the enrichment of thin sandy layers and clay–laminae surfaces with copper carbonates. This fluidisation episode likely also contributed to the copper enrichment of the carbonates in the overlying Tamjoute level by transporting aggressive fluids capable of generating karstic cavities and mineralising and silicifying the stromatolitic horizons. It is therefore highly probable that the combined effects of (i) a massive continental influx of copper during periods of relative sea-level fall, (ii) intense microbial activity within Ediacaran sedimentary ecosystems, and (iii) late-stage sediment liquefaction by fluids of still uncertain origin are responsible for the formation of the extensive Ediacaran stratiform copper district of the Western Anti-Atlas.

**Author Contributions:** Conceptualization, M.B.; methodology, M.B.; software, M.B. and M.A.; validation, M.A., N.I., M.O., A.E. and M.I.; formal analysis, M.B., A.M., A.B., A.W. and H.E.-B.; investigation, M.B., A.M., A.B. and H.E.-B.; resources, M.B., A.M. and A.B.; data curation, M.B., A.M. and A.B.; writing—original draft preparation, M.B.; writing—review and editing, A.M., A.B., M.A., N.I., M.O., A.E., A.W. and M.I.; visualization, M.B. and M.A.; supervision, A.E.; project administration, A.E.; funding acquisition, M.B. All authors have read and agreed to the published version of the manuscript.

**Funding:** This research received no external funding.

**Data Availability Statement:** The original contributions presented in this study are included in the article. Further inquiries can be directed to the corresponding author.

**Acknowledgments:** This study is part of the PhD thesis of the first author (M.B.) at Ibnou Zohr University, Morocco. In addition, the first author thanks the Centre National pour la Recherche Scientifique et Technique (CNRST) in Rabat, Morocco, for support under the PhD-Associate Scholarship program. The three anonymous reviewers are gratefully acknowledged for their constructive comments, which greatly improved the quality of this manuscript.

**Conflicts of Interest:** Authors Atmane Madi and Abdelilah Benhammou were employed by the company MANAGEM Group. The authors declare that the research was conducted independently and that their affiliations did not influence the scientific outcomes of the study. All co-authors declare no conflicts of interest.

## References


1. Huang, J.G.; Ren, T.; Zou, H.J. Genesis of Xinzhai Sandstone-type Copper Deposit in Northern Laos: Geological and Geochemical Evidence. *J. Earth Sci.* **2019**, *30*, 95–108. [CrossRef]
2. Maghfouri, S.; Movahednia, M.; Rastad, E.; Mahdavi, A.; Borg, G.; Hosseinzadeh, M.R.; Mousivand, F. Metallogeny and temporal–spatial distribution of sediment-hosted stratabound copper (SSC-type) deposits in Iran; implications for future exploration. *Ore Geol. Rev.* **2020**, *127*, 103834. [CrossRef]
3. Zhang, L.; Ye, L.; Yu, Z.S.; Shuai, L.; Liu, Z.Q.; Guan, G. Geological characteristics and geochemical significance of Silurian sandstone-type copper deposit in the northwestern margin of Tarim Basin. *Min. Resour. Geol.* **2021**, *35*, 186–193, (in Chinese with English abstract).
4. Shi, L.Q.; Qua, X.Y.; Zavala, C.; Li, Y. Metallogenic model of sandstone-hosted copper deposits: A case study from the Paleogene in Jiashi area, northwestern China. *J. Paleogeogr.* **2025**, *14*, 105–125. [CrossRef]
5. Brown, A.C. World-class sediment-hosted stratiform copper deposits: Characteristics, genetic concepts and metallotects. *Aust. J. Earth Sci.* **1997**, *44*, 317–328. [CrossRef]
6. Saintilan, N.J.; Selby, D.; Creaser, R.A.; Dewaele, S. Sulphide Re-Os geochronology links orogenesis, salt and Cu-Co ores in the Central African Copperbelt. *Sci. Rep.* **2018**, *8*, 14946. [CrossRef] [PubMed]
7. Perelló, J.; Clifford, J.A.; Creaser, R.A.; Valencia, V.A. An example of synorogenic sediment-hosted copper mineralization: Geologic and geochronologic evidence from the paleoproterozoic Nussir deposit, Finnmark, Arctic Norway. *Econ. Geol.* **2015**, *110*, 677–689. [CrossRef]
8. El Desouky, H.A.; Muchez, P.; Boyce, A.J.; Schneider, J.; Cailteux, J.L.H.; Dewaele, S.; von Quadt, A. Genesis of sediment-hosted stratiform copper–cobalt mineralization at Luiswishi and Kamoto, Katanga Copperbelt (Democratic Republic of Congo). *Miner. Depos.* **2010**, *45*, 735–763. [CrossRef]
9. Mouttaqi, A. Hydrothermalisme et Minéralisations en Relation Avec le Rifting Protérozoïque Supérieur: Exemple du Gisement de Cuivre de Bleïda (Anti-Atlas, Maroc). Dissertation Thesis, Cadi Ayyad University, Marrakech, Morocco, 1997. (In French)
10. Mouttaqi, A.; Sagon, J.P. Le gisement de cuivre de Bleïda (Anti-Atlas central); Une interférence entre les processus de remplacement et d'exhalaison dans un contexte de rift. *Chron. Rech. Min.* **1999**, *536–537*, 5–21. (In French)
11. Maacha, L. Études métallogéniques et géophysiques des minéralisations cobaltifères et cuprifères de Bou-Azzer El Graara, Anti-Atlas, Maroc. Ph.D. Thesis, Cadi Ayyad University, Marrakech, Morocco, 2013. (In French)
12. Maacha, L.; El Ghorfi, M.; Zouhair, M.; Sadiqqi, O.; Soulaimani, A. Minéralisations sulfurées de cuivre de la série de plateforme de Bleïda boutonnière de Bou Azzer-El Grâara (Anti-Atlas occidental). In *Actes du 8ème Colloque International du Magmatisme, Métamorphisme et Minéralisations Associées (3MA)*; Ibouh, H., Ed.; Notes et Mémoires du Service Géologique: Rabat, Morocco, 2015; Volume 579, pp. 125–131. (In French)
13. Jabbour, M.; Ilmen, S.; Ikenne, M.; Haissen, F.; Moundi, Y.; Karfal, A.; Souhassou, M.; Bouskri, I.; Maacha, L. Geological and structural study of the Co–Ni Arsenide deposit of Aghbar (Bou Azzer–El Graâra Inlier, Central Anti-Atlas, Morocco): Implications for mineral exploration. *Ecol. Eng. Environ. Technol.* **2025**, *26*, 303–320. [CrossRef] [PubMed]
14. Jabbour, M.; Ilmen, S.; Ikenne, M.; Zoheir, B.; Souhassou, M.; Bouskri, I.; El-Masoudy, A.; Prokopyev, I.; Oulhaj, M.; Ait Addi, M.; et al. Structural and Geochemical Controls on Copper Mineralization in the Aït Abdellah Deposit, Bou Azzer-El Graara Inlier, Anti-Atlas, Morocco. *Minerals* **2025**, *15*, 545. [CrossRef]
15. Chazan, W. Les gisements stratiformes plombo-zincifères de l'Infracambrien de l'Anti-Atlas occidental (Maroc). *Notes Mém. Serv. Géol. Maroc* **1954**, *120*, 97–126. (In French) [CrossRef]
16. Chazan, W.; Fauvelet, E. Les gîtes stratiformes de cuivre de l'Anti-Atlas occidental. I: Lithologie sédimentologique. In *Symposium sur les Gisements Stratiformes de Cuivre en Afrique*; Association des Services Géologiques Africains: Paris, France, 1962; pp. 43–52. (In French)
17. Pouit, G. Paléogéographie et répartition des minéralisations stratiformes de cuivre dans l'Anti-Atlas occidental. *Chron. Mines Rech. Min.* **1966**, *34*, 279–289. (In French)
18. Oummouch, A.; Essaifi, A.; Zayane, R.; Maddi, O.; Zouhair, M.; Maacha, L. Geology and Metallogenesis of the Sediment-Hosted Cu-Ag Deposit of Tizert (Igherm Inlier, Anti-Atlas Copperbelt, Morocco). *Geofluids* **2017**, *2017*, 7508484. [CrossRef]
19. Ouchchen, M.; Abia, E.H.; Soulaimani, A.; Abioui, M.; Lutz, B.; Benssaou, M.; Abdelrahman, K.; Abu-Alam, T.; Echogdali, F.Z.; Boutaleb, S. The Missing Link in the Genesis of the Lower Paleozoic Copper Deposits of the Anti-Atlas (Morocco): The Late Triassic Central Atlantic Magmatic Province Event. *Minerals* **2023**, *13*, 488. [CrossRef]

20. Bourque, H.; Barbanson, L.; Sizaret, S.; Branquet, Y.; Ramboz, C.; Ennaciri, A.; El Ghorfi, M.; Badra, L. Copper mineralization in Adoudounian cover of the BouAzzer-El Graara (Anti-Atlas, Morocco): Tectono stratigraphic controls. In Proceedings of the 13th SGA Biennal Meeting, Nancy, France, 24–27 August 2015. (In French)
21. Bourque, H.; Barbanson, L.; Sizaret, S.; Branquet, Y.; Ramboz, C.; Ennaciri, A.; Badra, L. A contribution to the synsedimentary versus epigenetic origin of the Cu mineralizations hosted by terminal Neoproterozoic to Cambrian formations of the Bou Azzer–El Graara inlier: New insights from the Jbel Laassel deposit (Anti Atlas, Morocco). *J. Afr. Earth Sci.* **2025**, *107*, 108–118. [CrossRef]
22. Bouskri, I.; Ilmen, S.; Souhassou, M.; Ikenne, M.; Zoheir, B.; Hajjar, Z.; Maacha, L.; Benzougagh, B.; Kader, S.; Jabbour, M.; et al. Geological setting, mineralogy, and isotopic characterization of the Jbel N'Zourk copper deposit, central Anti-Atlas, Morocco. *Ore Geol. Rev.* **2025**, *179*, 106533. [CrossRef]
23. Kharis, A.; Aissa, M.; Baidder, L.; Ouguir, H.; Mahmoudi, A.; Zouhair, M.; Ouadjo, A. Oumjrane-Bou Nahas, une mine de cuivre dans l'Ordovicien supérieur du Maider. In *Nouveaux Guides Géologiques et Miniers du Maroc, Principales Mines du Maroc*; Mouttaqi, A., Rjimati, E.C., Maacha, L., Michard, A., Soulaimani, A., Ibouh, H., Eds.; Notes et Mémoires du Service Géologique du Maroc: Rabat, Morocco, 2011; Volume 9, pp. 65–71. (In French)
24. Anthonioz, P.; Bahi, L.; Khalek, M. Un cas d'accumulation métallifère de type karstique dans un milieu carbonaté discontinu: Gîte cuprifère d'Amadouz (Anti-Atlas occidental, Maroc). *C.R. Acad. Sci. Paris* **1979**, *288*, 1251–1253.
25. Poot, J.; Verhaert, M.; Dekoninck, A.; Oummouch, A.; El Basbas, A.; Maacha, L.; Yans, J. Characterization of weathering processes of the giant copper deposit of Tizert (Igherm Inlier, Anti-Atlas, Morocco). *Minerals* **2020**, *10*, 620. [CrossRef]
26. McConachie, B.A.; Dunster, J.N. Sequence stratigraphy of the Bowthorn block in the northern Mount Isa basin, Australia: Implications for the base-metal mineralization process. *Geology* **1996**, *24*, 155–158. [CrossRef]
27. Ruffell, A.H.; Moles, N.R.; Parnell, J. Characterisation and prediction of sediment-hosted ore deposits using sequence stratigraphy. *Ore Geol. Rev.* **1998**, *12*, 207–223. [CrossRef]
28. Michard, A.; Saddiqi, O.; Chalouan, A.; Frizon de Lamotte, D. *Continental Evolution: The Geology of Morocco*; Springer: Berlin/Heidelberg, Germany, 2008. [CrossRef]
29. Ruiz, G.M.H.; Sebti, S.; Negro, F.; Saddiqi, O.; Frizon de Lamotte, D.; Stockli, D.; Foeken, J.; Stuart, F.; Barbarand, J.; Schaer, J.P. From central Atlantic continental rift to Neogene uplift-western Anti-Atlas (Morocco). *Terra Nova* **2011**, *23*, 35–41. [CrossRef]
30. Maloof, A.C.; Ramezani, J.; Bowring, S.A.; Fike, D.A.; Porter, S.M.; Mazouad, M. Constraints on early Cambrian carbon cycling from the duration of the Nemakit-Daldynian–Tommotian boundary $\delta^{13}C$ shift, Morocco. *Geology* **2010**, *38*, 623–626. [CrossRef]
31. Xiong, Y.; Chen, B.; Sun, X.; Chen, K.; Chraiki, I.; Yang, A.; Hu, C.; Sun, Z.; Pan, B.; Yang, C.; et al. Integrated analyses of the Ediacaran-Cambrian boundary sequence in northern Gondwana (Anti-Atlas platform, Morocco). *Gondwana Res.* **2025**, *145*, 79–106. [CrossRef]
32. Benssaou, M.; Hamoumi, N. Les microbialites de l'Anti-Atlas occidental (Maroc): Marqueurs stratigraphiques et témoins des changements environnementaux au Cambrien inférieur. *C.R. Géosci.* **2004**, *336*, 109–116. [CrossRef]
33. Gasquet, D.; Ennih, N.; Liégeois, J.-P.; Soulaimani, A.; Michard, A. The Pan-African Belt. In *Continental Evolution: The Geology of Morocco*; Michard, A., Saddiqi, O., Chalouan, A., Frizon Lamotte, D., Eds.; Springer: Berlin/Heidelberg, Germany, 2008. [CrossRef]
34. Soulaimani, A.; Ouanaimi, H.; Saddiqi, O.; Baidder, L.; Michard, A. The Anti-Atlas Pan African Belt (Morocco): Overview and pending questions. *Comptes Rendus Géosci.* **2018**, *350*, 279–288. [CrossRef]
35. Harms, J.C.; Southard, J.B.; Spearing, D.R.; Walker, R.G. *Depositional Environments as Interpreted from Primary Sedimentary Structures and Stratification Sequences*; SEPM Short Course No. 2; SEPM Society for Sedimentary Geology: Dallas, TX, USA, 1975. [CrossRef]
36. Reineck, H.E.; Singh, I.B. *Depositional Sedimentary Environments*, 2nd ed.; Springer: Berlin/Heidelberg, Germany, 1980. [CrossRef]
37. Einsele, G. *Sedimentary Basins: Evolution, Facies and Sediment Budget*; Springer: Berlin/Heidelberg, Germany, 2000. [CrossRef]
38. Miall, A.D. Recent developments in the study of fluvial facies models. In *Recent Developments in Fluvial Sedimentology*; Ethridge, F.G., Flores, R.M., Harvey, M.D., Eds.; SEPM Society for Sedimentary Geology: Tulsa, OK, USA, 1987; Volume 39. [CrossRef]
39. Nemec, W.; Steel, R.L. Alluvial and coastal conglomerates: Their significant features and some comments on gravelly mass flow deposits. In *Sedimentology of Gravels and Conglomerates*; Koster, E.H., Steel, R.J., Eds.; Canadian Society of Petroleum Geologists: Calgary, AB, Canada, 1987; Memoir 10; pp. 1–13.
40. Catuneanu, O. *Principles of Sequence Stratigraphy*; Elsevier: Amsterdam, The Netherlands, 2006.
41. Takahashi, T. Debris flow. *Annu. Rev. Fluid Mech.* **1981**, *13*, 57–77. [CrossRef]
42. Iverson, R.M. The debris-flow rheology myth. In *Proceedings of the International Conference on Debris-Flow Hazards Mitigation: Mechanics, Prediction, and Assessment, Davos, Switzerland, 10–12 September 2003*; Rickenmann, D., Chen, C.L., Eds.; Millpress: Rotterdam, The Netherlands, 2003; Volume 1, pp. 303–314.
43. Hampton, M.A. The role of subaqueous debris flow in generating turbidity currents. *J. Sedim. Res.* **1972**, *42*, 775–793. [CrossRef]
44. Walker, R.G. Generalized facies models for resedimented conglomerates of turbiditic association. *GSA Bull.* **1975**, *86*, 737–748. [CrossRef]

45. Middleton, G.V. Experiments on density and turbidity currents. III. Deposition of sediment. *Canad. J. Earth Sci.* **1967**, *4*, 475–505. [CrossRef]
46. Middleton, G.V. Sediment deposition from turbidity currents. *Ann. Rev. Earth Planet Sci.* **1993**, *21*, 89–114. [CrossRef]
47. Postma, G.; Cartigny, M.J.B. Supercritical and subcritical turbidity currents and their deposits–A synthesis. *Geology* **2014**, *42*, 987–990. [CrossRef]
48. Obermeier, F. Use of liquefaction-induced features for paleoseismic analysis—An overview of how seismic liquefaction features can be distinguished from other features and how their regional distribution and properties of source sediment can be used to infer the location and strength of Holocene paleo-earthquakes. *Eng. Geol.* **1996**, *44*, 1–76. [CrossRef]
49. Osborne, M.J.; Swarbrick, R.E. Mechanisms for generating overpressure in sedimentary basins: A reevaluation. *AAPG Bull.* **1997**, *81*, 1023–1041. [CrossRef]
50. Lorenz, J.C.; Teufel, L.W.; Warpinski, N.R. Regional fractures I: A mechanism for the formation of regional fractures at depth in flat-lying reservoirs. *AAPG Bull.* **1991**, *75*, 1714–1737. [CrossRef]
51. Cosgrove, J.W.; Hillier, R.D. Forced-fold development within Tertiary sediments of the Alba Field, UKCS: Evidence of differential compaction and post-depositional sandstone remobilisation. *Geol. Soc. Lond. Spec. Publ.* **2000**, *169*, 61–71. [CrossRef]
52. Lonergan, L.; Lee, N.; Johnson, H.D.; Jolly, R.J.H.; Cartwright, J.A. Remobilization and injection in deepwater depositional systems: Implications for reservoir architecture and prediction. In *Deep-Water Reservoirs of the World*; Wiemer, P., Ed.; SEPM Society for Sedimentary Geology: Tulsa, OK, USA, 2000; pp. 515–532. [CrossRef]
53. Jolly, R.J.H.; Lonergan, L. Mechanisms and controls on the formation of sand intrusions. *J. Geol. Soc.* **2002**, *159*, 605–617. [CrossRef]
54. Duranti, D.; Hurst, A. Fluidization and injection in the deep-water sandstones of the Eocene Alba Formation (UK North Sea). *Sedimentology* **2004**, *51*, 503–529. [CrossRef]
55. Dasgupta, P.; Chatterjee, A. Formation of water-escape structure during shock-induced fluidization: The role of permeability contrast. *J. Struct. Geol.* **2019**, *124*, 1–7. [CrossRef]
56. Leblanc, M. Appareil ignimbritique et minéralisation cuprifère: Alous (Anti-Atlas, Maroc). *Miner. Depos.* **1986**, *21*, 129–136. [CrossRef]
57. Maddi, A.; Baoutoul, H.; Maacha, L.; Ennaciri, A.; Soulaimani, A. La mine d'Agjgal au sud du Kerdous; considérations sur les gîtes stratoïdes de cuivre et argent de l'Anti-Atlas occidental et central. In *Nouveaux Guides Géologiques et Miniers du Maroc, Principales Mines du Maroc*; Mouttaqi, A., Rjimati, E.C., Maacha, L., Michard, A., Soulaimani, A., Eds.; Notes et Mémoires du Service Géologique du Maroc: Rabat, Morocco, 2011; Volume 9, pp. 151–156. (In French)
58. Achnin, H. Le Gisement Cuprifère Stratiforme de Tiferki (Boutonnière d'Irherm, Anti-Atlas, Maroc): Géologie Régionale, Minéralogie, Métallogénie et Géochimie. Ph.D. Thesis, Université de Strasbourg 1, Strasbourg, France, 1979. (In French)
59. Soulaimani, A.; Bouabdelli, M.; Piqué, A. L'extension continentale au Néo-Protérozoïque supérieur-Cambrien inférieur dans l'Anti-Atlas (Maroc). *Bull. Soc. Géol. Fr.* **2003**, *174*, 83–92. [CrossRef]
60. Bouda, A.; Choubert, G.; Faure-Muret, A. *Essai de Stratigraphie de la Couverture Sédimentaire de l'Anti-Atlas: Adoudounien-Cambrien Inférieur*; Notes et Mémoires du Service Géologique: Rabat, Morocco, 1979. (In French)
61. Benziane, F.; Yazidi, A.; Prost, A.E. Le passage du Précambrien au Cambrien précoce volcanique et sédimentaire de l'Anti-Atlas oriental, comparaison avec l'Anti-Atlas occidental. *Bull. Soc. Géol. Fr.* **1983**, *7*, 549–556. [CrossRef]
62. Zavala, C.; Pan, S.X. Hyperpycnal flows and hyperpycnites: Origin and distinctive characteristics. *Lithol. Reserv.* **2018**, *30*, 1–27. [CrossRef]
63. Baudin, F.; Tribovillard, N.; Trichet, J. *Géologie de la Matière Organique*; EDP Sciences: Les Ulis, France, 2017. (In French)
64. Riding, R.E.; Awramik, S.M. *Microbial Sediment*; Springer: Berlin/Heidelberg, Germany, 2000. [CrossRef]
65. Sarkar, S.; Banerjee, S.; Chakraborty, P.P. Microbial Mat Structures and role of microbes in Precambrian siliciclastic sedimentation: Evidence from Indian Proterozoic basins. *Episodes* **2020**, *43*, 164–173. [CrossRef]
66. Sarkara, S.; Banerjeeb, S.; Samantac, P.; Chakrabortya, N.; Chakrabortyd, P.P.; Mukhopadhyayc, S.; Singhd, A.K. Microbial mat records in siliciclastic rocks: Examples from Four Indian Proterozoic basins and their modern equivalents in Gulf of Cambay. *J. Asian Earth Sci.* **2014**, *91*, 362–377. [CrossRef]
67. Ferris, F.G. Metallic ion interactions with the outer membrane of gram-negative bacteria. In *Metal Ions and Bacteria*; Beveridge, T.J., Doyle, R.J., Eds.; John Wiley and Sons: New York, NY, USA, 1989; pp. 295–323.
68. Ferris, F.G.; Beveridge, T.J.; Fyfe, W.S. Iron–silica crystallite nucleation by bacteria in a geothermal sediment. *Nature* **1986**, *320*, 609–611. [CrossRef]
69. Ferris, F.G.; Fyfe, W.S.; Beveridge, T.J. Metallic ion binding by Bacillus subtilis: Implications for the fossilization of microorganisms. *Geology* **1988**, *16*, 149–152. [CrossRef]
70. Ferris, F.G.; Schultze, S.; Witten, T.C.; Fyfe, W.S.; Beveridge, T.J. Metal interactions with microbial biofilms in acidic and neutral pH environments. *Appl. Environ. Microbiol.* **1989**, *55*, 1249–1257. [CrossRef] [PubMed]
71. Ehrlich, H.L. Microbes and metals. *Appl. Microbiol. Biotechnol.* **1997**, *48*, 687–692. [CrossRef]
72. Konhauser, K.O. Bacterial iron mineralisation in nature. *FEMS Microbiol. Rev.* **1997**, *20*, 315–326. [CrossRef]

73. Konhauser, K.O.; Jones, B.; Reysenbach, A.L.; Renaut, R.W. Hot spring sinters: Keys to understanding Earth's earliest life forms. *Can. J. Earth Sci.* **2003**, *40*, 1713–1724. [CrossRef]
74. Konhauser, K.O.; Phoenix, V.R.; Bottrell, S.H.; Adams, D.G.; Head, I.M. Microbial-silica interactions in Icelandic hot spring sinter: Possible analogues for some Precambrian siliceous stromatolites. *Sedimentology* **2001**, *48*, 415–433. [CrossRef]
75. Evans, D.J.A.; Phillips, E.R.; Hiemstra, J.F.; Auton, C.A. Subglacial till: Formation, sedimentary characteristics and classification. *Earth Sci. Rev.* **2006**, *78*, 115–176. [CrossRef]
76. Rijsdijk, K.F.; Owen, G.; Warren, W.P.; McCarroll, D.; van der Meer, J.J.M. Clastic dykes in over-consolidated tills: Evidence for subglacial hydrofracturing at Killiney Bay, eastern Ireland. *Sediment. Geol.* **1999**, *129*, 111–126. [CrossRef]
77. Squire, R.J.; Keays, R.R. The role of supermountain belts and climatic controls on the genesis of copper deposits in the Kupferschiefer and the Central African Copperbelt. *Miner. Depos.* **2024**, *59*, 717–732. [CrossRef]
78. Daly, M.C.; Zimba, M.; Purkiss, M.; Chibesakunda, F. The Inter-Cratonic Neoproterozoic Katangan Basin of Central Africa: Rift Basin Formation, Orogenic Inversion and Potential Fluid Pathways. *Tectonics* **2025**, *44*, e2025TC008955. [CrossRef]
79. Hayes, B.; Bédard, J.H.; Hryciuk, M.; Wing, B.; Nabelek, P.; MacDonald, W.D.; Lissenberg, C.J. Sulfide immiscibility induced by wall-rock assimilation in a fault-guided basaltic feeder system, Franklin Large Igneous Province, Victoria Island (Arctic Canada). *Econ. Geol.* **2015**, *110*, 1697–1717. [CrossRef]
80. Blundell, D.J.; Karnkowski, P.H.; Alderton, D.H.M.; Oszczepalski, S.; Kucha, H. Copper mineralization of the Polish Kupferschiefer—A proposed basement fault fracture system of fluid flow. *Econ. Geol.* **2003**, *98*, 1487–1495. [CrossRef]


**Disclaimer/Publisher's Note:** The statements, opinions and data contained in all publications are solely those of the individual author(s) and contributor(s) and not of MDPI and/or the editor(s). MDPI and/or the editor(s) disclaim responsibility for any injury to people or property resulting from any ideas, methods, instructions or products referred to in the content.